Journal of Geophysical Research: Biogeosciences

RESEARCH ARTICLE
10.1029/2017JG004348

Attributing the Carbon Cycle Impacts of CMIP5 Historical and Future Land Use and Land Cover Change in the Community Earth System Model (CESM1)

Peter J. Lawrence[1], **David M. Lawrence**[1], **and George C. Hurtt**[2]

[1]National Center for Atmospheric Research, Boulder, CO, USA, [2]Geographical Sciences, University of Maryland, College Park, MD, USA

Key Points:
- We systematically attribute the carbon cycle impacts of LULCC in the Community Earth System Model from flux and carbon pool calculations
- For the historical period CESM produced a cumulative Effective LULCC flux of 123 PgC Effective LULCC flux of 123 PgC to the atmosphere
- For the RCP 4.5 scenario, CESM was able to partially represent the mitigation effects of afforestation prescribed by GCAM

Supporting Information:
- Supporting Information S1

Correspondence to:
P. J. Lawrence,
lawrence@ucar.edu

Citation:
Lawrence, P. J., Lawrence, D. M., & Hurtt, G. C. (2018). Attributing the carbon cycle impacts of CMIP5 historical and future land use and land cover change in the Community Earth System Model (CESM1). *Journal of Geophysical Research: Biogeosciences*, *123*, 1732–1755. https://doi.org/10.1029/2017JG004348

Received 5 DEC 2017
Accepted 25 APR 2018
Accepted article online 4 MAY 2018
Published online 24 MAY 2018

Abstract Historical global land use and land cover change (LULCC) emissions of 160 PgC represent a third of all human CO_2 emissions from 1850 to 2010. Future land management decisions will have large impacts on the global carbon cycle, with scenarios ranging from continued deforestation and wood harvest to mitigation scenarios that reduce total emissions through afforestation and conversion to bioenergy. Here we present a systematic assessment of Community Earth System Model (CESM1) Coupled Model Intercomparison Project phase 5 (CMIP5) historic and projection simulations, with and without LULCC. For the historical period, CESM produced a Net LULCC flux of 123 PgC to the atmosphere, removing −130 PgC from ecosystems while increasing wood product pools by 7 PgC. Historical LULCC fluxes were equally divided between conversion and wood harvest fluxes. For the Representative Concentration Pathway (RCP) 4.5 afforestation scenario CESM produced a Net LULCC flux of 53 PgC to the atmosphere, removing −58 PgC out of the ecosystem and increasing wood product pools of 5 PgC. The afforestation offsets the Direct LULCC flux of 153 PgC with a negative Indirect LULCC flux of −94 PgC. For the RCP 8.5 high LULCC scenario, CESM produced a Net LULCC flux of 211 PgC, removing −227 PgC from ecosystems and increasing wood product pools of 15 PgC. The LULCC of the future RCP scenarios was dominated by wood harvest fluxes, which is a process that was not included in many of the CMIP5 models. The analysis framework also allowed the attribution of Indirect and Prior LULCC fluxes that offset the Direct LULCC fluxes in many cases.

1. Introduction

Historical land use and land cover change (LULCC) from wood harvest and clearing for agriculture and pasture have been major sources of human emissions of CO_2 to the atmosphere, with cumulative global estimates of 160 PgC representing a third of all human CO_2 emissions from 1850 to 2010 (Arneth et al., 2017; Canadell et al., 2007; Ciais et al., 2014; Houghton, 2003, 2010; D. M. Lawrence et al., 2016). Current-day LULCC fluxes continue to be a major contribution to atmospheric CO_2 with estimates of LULCC emissions totaling ~1 PgC/yr (Arneth et al., 2017; Arora & Boer, 2010; Houghton et al., 2012; Le Quere et al., 2015; Pan et al., 2011; van der Werf et al., 2009).

Future land management decisions will have large impacts on the global carbon cycle with scenarios of LULCC ranging from continued high rates of deforestation and wood harvest, leading to large carbon emissions to the atmosphere (Brovkin et al., 2013; Mahowald et al., 2016; Pongratz et al., 2014; Riahi et al., 2011) to mitigation scenarios that rely on land management to mitigate fossil fuel emissions through afforestation and bioenergy production (Canadell & Schulze, 2014; Smith et al., 2013; Thomson et al., 2011).

To investigate the climate impacts and uncertainties involved with LULCC, the Coupled Model Intercomparison Project phase 5 (CMIP5) included land cover change and wood harvest as a forcing for all of the historical and future Representative Concentration Pathway (RCP) climate projections. The prescription of the CMIP5 LULCC in the Community Earth System Model (CESM1) and the climate and carbon cycle response to LULCC in concert with other transient forcings are described in P. J. Lawrence et al. (2012). In these simulations, CESM produced a historical decrease of 61 PgC in terrestrial ecosystem carbon, as compared to an increase of 67 PgC in the reforestation scenario of RCP 4.5, and a loss of 30 PgC in the deforestation and high wood harvest scenario of RCP 8.5.

Brovkin et al. (2013), however, demonstrated that direct attribution of carbon cycle and climate changes due to LULCC was not possible in the CMIP5 experiments due to the confounding influences of changing climate and CO_2 fertilization on the terrestrial ecosystem at the same time as the LULCC was occurring. Additional studies by Arneth et al. (2017), Mahowald et al. (2016), and Pongratz et al. (2014) have also raised the issue that the Direct LULCC carbon fluxes calculated by Earth system models do not account for the Indirect and Feedback carbon fluxes associated with carbon uptake from new or restored forests, from losses of potential carbon sinks that the cleared forests would have had from increased productivity with rising atmospheric CO_2 in the absence of the LULCC or from changes in soil and litter carbon associated with the new land use.

All of these studies argued that the full impact of LULCC on the terrestrial carbon cycle can only be assessed by comparing full transient simulations with LULCC to the equivalent simulations run without LULCC and then evaluating the differences in the carbon cycle between the simulations. Constant land use and land cover simulations were performed for a subset of six of the CMIP5 climate models as a side project by Brovkin et al. (2013), but the CESM was not included as part of that study due to resource limitations at that time. Here we report on results from ensembles of historical and RCP 4.5 and RCP 8.5 future simulations with full transient forcing without LULCC for comparison with the original CESM CMIP5 simulations with LULCC.

In this study we present a flux-based LULCC assessment framework that allows direct attribution of changes in carbon fluxes and pools to the Direct, Indirect, Ecosystem, Net, Prior, and Feedback components of LULCC fluxes (defined further on), explicitly from terms recorded on CESM output files. The purpose of the LULCC framework is to systematically attribute how LULCC actions impact the fluxes of carbon to the atmosphere and how LULCC actions impact the state and function of terrestrial ecosystems.

For our investigation, we evaluated RCP 4.5 and RCP 8.5 as they represent the most extreme LULCC scenarios in the CMIP5 protocol with widespread afforestation and deforestation, respectively (van Vuuren et al., 2011). The comparison of the same fully coupled transient simulations with and without LULCC provides insight into the range of climate and carbon cycle responses that are possible using the alternative plausible Integrated Assessment Model futures of CMIP5. The experimental framework allows for the quantification of the net flux of carbon to the atmosphere as a result of LULCC and the change in ecosystem state and function in response to the LULCC.

2. Data and Methods

2.1. Experimental Design

The CESM version 1.0 simulations performed in this study are transient fully coupled simulations with forcing prescribed from the CMIP5 protocol following Taylor et al. (2009). As in the Brovkin et al. (2013) study, all of the CESM simulations in this study use prescribed atmospheric concentrations of radiative gases associated with the scenario rather than prognostically simulating concentrations through a fully coupled carbon cycle.

The CESM configuration used in this study is the same configuration as used in the CMIP5 original CESM simulations described by Lindsay et al. (2014), with the atmospheric concentration of CO_2 prescribed. This model configuration consists of the Community Land Model with the Carbon Nitrogen option (CLM4CN) as described by D. M. Lawrence et al. (2012), with the other coupled components of the Community Atmosphere Model (CAM4), the Parallel Ocean Program (POP2), and the Community Ice Code (CICE4) as described by Gent and Danabasoglu (2011). All simulations were run at the finite volume $0.9 \times 1.25°$ resolution for the land and atmosphere and at the 1° resolution for the ocean and sea ice.

Three historical transient and no LULCC ensemble simulations were started as simulation pairs from initial conditions taken from the CESM 1850 control simulation from the years 863, 864, and 865 as described in Lindsay et al. (2014). The historical simulations were run from 1850 to 2005 following the CMIP5 protocol for all other forcings. The RCP transient and no LULCC ensemble simulations were started from the beginning of 2005 grouped by the initial conditions from the end of the three historical full transient simulations. The RCP simulations were run from 2005 to 2100 following their respective forcing pathways.

2.2. Framework for Direct, Indirect, Ecosystem, Net, Prior, and Feedback LULCC Fluxes

The LULCC analysis framework follows the work and definitions provided by Arneth et al. (2017), Brovkin et al. (2013), Canadell et al. (2007), Gasser and Ciais (2013), Le Quere et al. (2015), Mahowald et al. (2016),

Pongratz et al. (2014), and Watson et al. (2000). This framework extends the fluxes and carbon pools shown in Figure 2a of P. J. Lawrence et al. (2012) with the addition of net biosphere production (NBP) as defined in Watson et al. (2000).

Here the definition of NBP is "the net production of organic matter in a region containing a range of ecosystems (a biome) and includes, in addition to heterotrophic respiration, other processes leading to loss of living and dead organic matter (harvest, forest clearance, and fire, etc.)." This can be written as the uptake carbon from net ecosystem production (NEP) minus the loss of carbon from wildfires (Fire) and the direct activities of LULCC ($LULCC_{DIRECT}$):

$$NBP = NEP–Fire–LULCC_{DIRECT} \quad (1)$$

The NEP term is defined as the ecosystem photosynthesis uptake of carbon through net primary productivity (NPP) minus the loss of carbon through heterotrophic respiration (HR) from the decay leaf litter, coarse woody debris, and soil organic matter. This can be written as

$$NEP = NPP–HR \quad (2)$$

The first component of the LULCC analysis framework is the Direct LULCC flux, which applies to the loss of carbon from the land associated with Direct actions such as land cover transformation or wood harvest. The Direct LULCC flux is equivalent to the Instantaneous LULCC flux in equation (3) of Pongratz et al. (2014).

For CESM land cover transformation there is a component of the carbon that is directly released to the atmosphere through fires and rapid decay ($Conversion_{ATM}$), and there is a component that is harvested and transferred to wood product pools ($Conversion_{PROD}$). For the process of wood harvest where timber is removed from the ecosystem and the ecosystem remains as a forest or savanna, there is only the carbon taken out as wood products, with the remaining disturbed carbon staying in the ecosystem as fluxes to litter and coarse woody debris (also known as slash). In CESM the Direct LULCC ($LULCC_{DIRECT}$) flux is defined as

$$LULCC_{DIRECT} = Conversion_{ATM} + Conversion_{PROD} + Wood\ Harvest \quad (3)$$

For this study the Direct LULCC is performed without LULCC flux driven atmospheric CO_2 feedbacks as the transient atmospheric CO_2 concentration is prescribed from CMIP5 forcing. As detailed later the Feedbacks component of the framework, the LULCC CO_2 feedback can be evaluated by comparing the Direct LULCC with prescribed CO_2 compared to the Direct LULCC with coupled prognostic CO_2.

The second component of the framework is the Indirect LULCC flux, which arises from the LULCC-driven changes in ecosystem state and function compared with their state and function in the absence of LULCC. The Indirect LULCC flux is equivalent to the Legacy flux *L* in equation (3) of Pongratz et al. (2014) with the inclusion of wildfire, which is missing in the original framework.

In this manner the Indirect LULCC flux accounts for both the loss of additional sink capacity due to the loss of potential carbon sinks from deforestation, as well as the increased uptake of carbon due to afforestation or recovery from disturbance. This also captures changes in heterotrophic respiration, and fire after LULCC removes large amounts of carbon from the ecosystem. In Earth system models the transient changes in vegetation state and function due to LULCC can only be calculated by simulating the carbon cycle with LULCC (LU) and then comparing to the same simulations without LULCC (NOLU). As with the Direct LULCC flux, this flux can be calculated with or without LULCC CO_2 feedbacks. The Indirect LULCC fluxes ($LULCC_{INDIRECT}$) are defined as

$$LULCC_{INDIRECT} = \Delta HR_{LU-NOLU} + \Delta Fire_{LU-NOLU} - \Delta NPP_{LU-NOLU.} \quad (4)$$

The third component of the framework is the Ecosystem LULCC flux, which is the combined impact of the Direct and Indirect LULCC fluxes of carbon out of terrestrial ecosystems. The Ecosystem LULCC flux is different to the Net LULCC flux to the atmosphere in equation (2) in Pongratz et al. (2014) due to the inclusion of wildfire in CESM. The Ecosystem LULCC Flux ($LULCC_{ECOSYS}$) is defined as

$$LULCC_{ECOSYS} = LULCC_{DIRECT} + LULCC_{INDIRECT.} \quad (5)$$

The forth component of the framework is the Net LULCC flux, which is different to the Net LULCC flux in Pongratz et al. (2014) due to the inclusion of LULCC-driven changes in wildfire and the delayed release of

wood product carbon in CESM. The Net LULCC flux is calculated as the Ecosystem LULCC flux minus the growth rate of the wood product pools (GrowthProdC). The Net LULCC flux ($LULCC_{NET}$) is defined as

$$LULCC_{NET} = LULCC_{ECOSYS} - GrowthProdC \quad (6)$$

The growth rate of the wood product pools is the difference in the rate of transfer of carbon to the product pools from Direct LULCC and the rate of decay of carbon out of the product pools as paper and wood products are discarded and break down (DecayProdC). In CESM wood products are divided into two pools, one with a 10-year decay rate and the other with a 100-year decay rate. The rate of change of the wood product pools in CESM is defined as

$$GrowthProdC = Conversion_{PROD} + Wood\ Harvest - DecayProdC \quad (7)$$

The impact of the Ecosystem and Net LULCC fluxes on carbon pools over a scenario can be calculated as the cumulative totals of the fluxes. The cumulative Ecosystem LULCC flux out of the terrestrial ecosystem is equal to the difference in total ecosystem carbon (TotalEcoSysC) between the LULCC and no LULCC simulations at the end of the period. The Net LULCC flux, however, is equal to the difference in total ecosystem carbon between the simulations minus the change in the size of the product pools over the LULCC simulation period. The cumulative LULCC flux impacts are defined as

$$\int_{start}^{end} LULCC_{ECOSYS}\, dt = \Delta TotalEcoSysC_{NOLU-LU} \quad (8)$$

$$\int_{start}^{end} LULCC_{NET}\, dt = \Delta TotalEcoSysC_{NOLU-LU} - \Delta ProductC_{LU\ end-start} \quad (9)$$

The Ecosystem and Net LULCC fluxes do not include the ongoing Indirect LULCC fluxes that have resulted from LULCC prior to the beginning of the simulations. To assess these impacts, the Prior LULCC fluxes can be calculated as the Indirect LULCC flux of the no LULCC transient simulations compared to simulations with no LULCC and the vegetation that would have been present without the LULCC from before the beginning of the scenario. The Prior LULCC is defined as

$$LULCC_{PRIOR} = \Delta NPP_{NOLUPRIOR-NOLU} - \Delta HR_{NOLUPRIOR-NOLU} - \Delta Fire_{NOLUPRIOR-NOLU} \quad (10)$$

The Prior LULCC flux is a more generalized representation of the managed, natural, and potential land-type subscripts (m, n, and p) used in Pongratz et al. (2014), which can be directly applied in CESM simulations. This more generalized representation allows for attribution of ongoing impacts of LULCC that occurred prior to the start of the investigated time period regardless of whether they are managed, natural, or potential. In this manner the Prior LULCC captures ongoing changes in NBP due the loss of potential sinks from previous deforestation or the continued uptake of carbon due to previous afforestation and recovery from disturbance.

As previously mentioned, the LULCC analysis framework also allows for feedback analysis of the Direct, Ecosystem, and Net LULCC fluxes with and without coupling to an active component within the Earth system model. An example of this feedback analysis involves evaluating the differences in the Net LULCC fluxes in fully coupled Earth system simulations with prescribed atmospheric CO_2 concentrations compared to equivalent simulations with emission-driven atmospheric CO_2, as performed in Mahowald et al. (2016). In this case the CO_2 concentration evolves as a result of the emissions and sinks of the carbon cycle and the carbon cycle feedbacks are then explicitly explored as differences between the two experimental configurations. The Feedback LULCC ($LUCC_{FEEDBACK}$) fluxes are defined as

$$LULCC_{FEEDBACK} = LULCC_{EFFECTIVE\ COUPLED} - LULCC_{EFFECTIVE\ PRESCRIBED} \quad (11)$$

The Feedback LULCC is a generic term depending on which active component of CESM is being turned on or off in the experimental design. The generic nature of this component allows for exploration of the range of configurations described in Pongratz et al. (2014) including LULCC under constant CO_2 and climate. As previously mentioned, we do not investigate the Feedback LULCC terms of the CESM simulations of this study as the atmospheric CO_2 concentrations are prescribed from CMIP5; however, this component is presented here for completeness of the assessment framework.

The final component of the LULCC framework attributes how LULCC impacts the net biosphere flux from the land to the atmosphere and the residual sink from the atmosphere to the land. For the net biosphere flux we apply the Definition 1 of Net LULCC flux ($ELUC_{def1}$) from Gasser and Ciais (2013), which is an extension of equations (1) and (3) from Pongratz et al. (2014) to include wildfire and the growth rate of the wood products pool that are both explicitly represented in CESM. In CESM the net biosphere flux from the LULCC simulation ($NetFlux_{LU}$) and the no LULCC simulation ($NetFlux_{NOLU}$) are defined as

$$NetFlux_{LU} = LULCC_{DIRECT} + HR_{LU} + Fire_{LU} - NPP_{LU} - GrowthProdC_{LU} \quad (12)$$

$$NetFlux_{NOLU} = HR_{NOLU} + Fire_{NOLU} - NPP_{NOLU} \quad (13)$$

and from equation (17) of Gasser and Ciais (2013) the Net LULCC flux is defined as

$$\begin{aligned} LULCC_{NET} &= NetFlux_{LU} - NetFlux_{NOLU} \\ &= LULCC_{DIRECT} + \Delta HR_{LU-NOLU} + \Delta Fire_{LU-NOLU} - \Delta NPP_{LU-NOLU} - GrowthProdC_{LU} \\ &= LULCC_{DIRECT} + LULCC_{INDIRECT} - GrowthProdC_{LU} \end{aligned} \quad (14)$$

which is consistent with equations (5) and (6).

For the residual sink we use the original definition of the term provided by Canadell et al. (2007) and Watson et al. (2000) as the potential for ecosystems to take up carbon from the atmosphere once all direct fluxes are accounted for. Both Gasser and Ciais (2013) and Pongratz et al. (2014) represent the residual sink of the LULCC simulations by subtracting out the Net LULCC flux from the net biosphere flux. The result of this is to represent the residual sink of both the LULCC and no LULCC simulation with the same value taken from the no LULCC simulation. This has the problem of providing no information on how LULCC has changed the potential for the land surface to take up carbon. Here we define the residual sink (ResSink) as the amount of carbon that is taken up by the land surface once the Direct LULCC flux is accounted for. The residual sinks of the LULCC ($ResSink_{LU}$) and the no LULCC ($ResSink_{LU}$) are defined as

$$ResSink_{LU} = LULCC_{DIRECT} - NetFlux_{LU} = GrowthProdC_{LU} + NPP_{LU} - HR_{LU} - Fire_{LU} \quad (15)$$

$$ResSink_{NOLU} = -NetFlux_{NOLU} = NPP_{NOLU} - HR_{NOLU} - Fire_{NOLU} \quad (16)$$

This then provides a definition for the LULCC-driven changes in the residual sink by comparing the LULCC and no LULCC simulations as

$$\Delta ResSink_{LU-NOLU} = GrowthProdC + \Delta NPP_{LU-NOLU} - \Delta HR_{LU-NOLU} - \Delta Fire_{LU-NOLU} \quad (17)$$

and substituting in from equation (4) this can be written as

$$\Delta ResSink_{LU-NOLU} = GrowthProdC - LULCC_{INDIRECT} \quad (18)$$

This final component demonstrates that the LULCC impacts on the fluxes from the land to the atmosphere can be expressed as the Direct LULCC flux plus LULCC-driven changes in the residual sink. The changes in the residual sink can then be expressed as the growth rate of wood product pools minus the Indirect LULCC flux, which also is consistent with the definition of the Net LULCC flux.

2.3. Specified Annual LULCC and Wood Harvest

The LULCC for each simulation was prescribed according to the CMIP5 historical and RCP trajectories as described in Hurtt et al. (2011) and P. J. Lawrence et al. (2012). For the no LULCC simulations vegetation and land use distributions were taken from 1850 for the historical simulations and from 2005 for the RCP future simulations. For both the historical and RCP time periods wood harvest in the no LULCC simulations was maintained at zero for the entire period. To address residual product pool carbon in the initial conditions of the RCP simulations, these pools are set to zero in the RCP no LULCC simulations.

To calculate the Historical Prior LULCC fluxes, a Potential Vegetation no LULCC time series was prescribed with vegetation distributions that represented 100% Primary Vegetation of Hurtt et al. (2011) making them very close to the initial vegetation distributions of the CESM1 last millennium simulations (Landrum et al., 2013). For the RCP Prior LULCC calculation an 1850 no LULCC time series was prescribed with 1850 vegetation

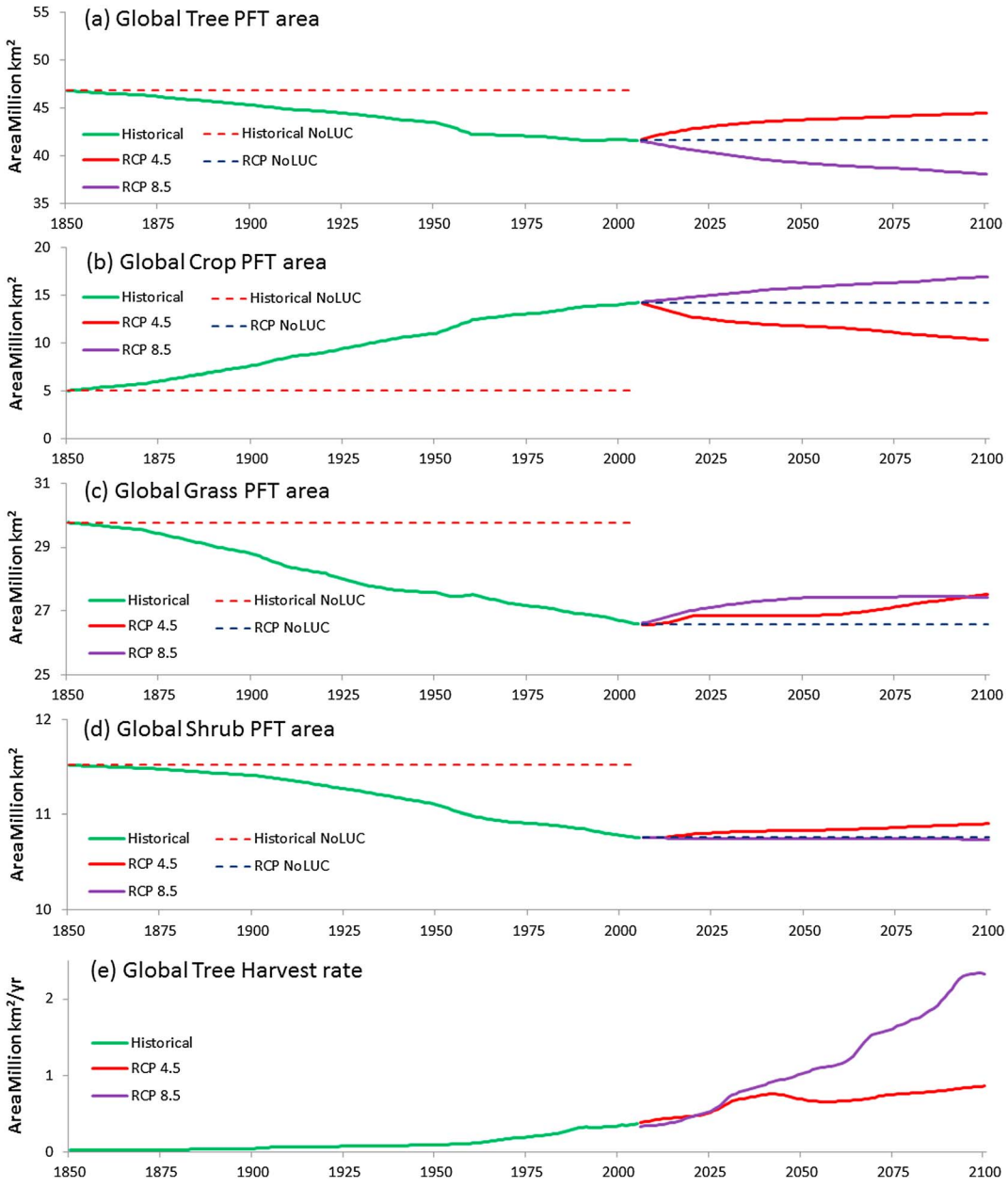

Figure 1. Global LULCC and no LULCC time series for (a) trees, (b) crops, (c) grasses, (d) shrubs, and (e) tree wood harvest rate.

until 2100. The initial conditions of the Historical Prior no LULCC simulations were generated from extended spun-up versions of the 1850 initial conditions. The initial conditions of the RCP 1850 no LULCC simulations were taken from the end of the Historical no LULCC simulations.

3. Results

3.1. Land Use and Land Cover Change Time Series and Carbon Cycle Analysis in CESM

Global and regional time series of the historical, RCP 4.5, and RCP 8.5 vegetation distributions and wood harvest as compared to the values from Hurtt et al. (2011) are shown in Figures 1 and 2 and Table 1. Following the LULCC assessment framework defined in section 2.2, the CESM LULCC carbon fluxes and the changes to other terrestrial carbon cycle fluxes are shown in Figures 3–5 and Tables 2 and 3. Global maps of Direct,

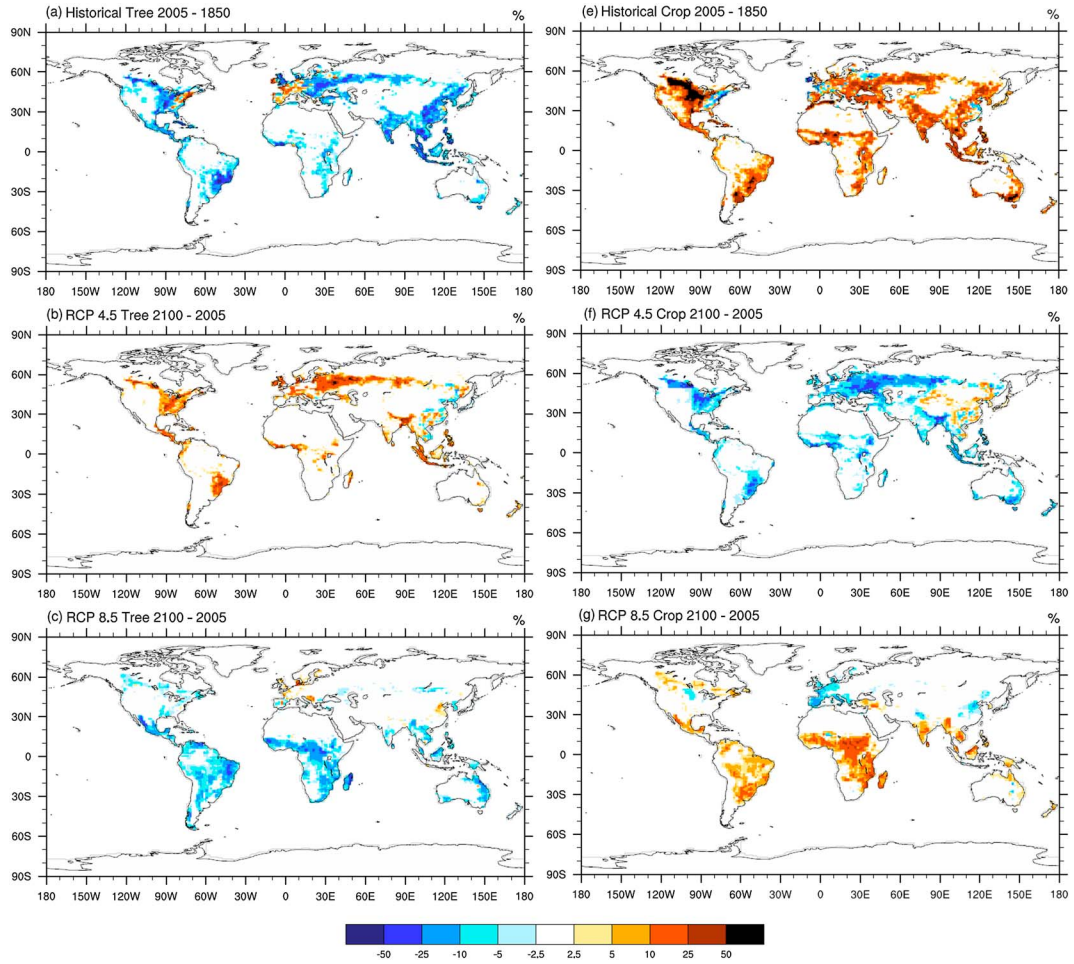

Figure 2. Cumulative land cover change for trees and crops for historical (1850 to 2005), RCP 4.5 (2006 to 2100), and RCP 8.5 (2006 to 2100) time periods as percentage of land area.

Indirect, Net, and Prior LULCC fluxes are shown in Figures 6 and 7. Additional difference maps for conversion, wood harvest, NPP, HR, fire, NEP, residual sink, and NBP fluxes are shown in supporting information Figures S1–S4.

Further assessment of the LULCC impacts on the global carbon cycle is shown through changes in the CESM ecosystem and product carbon pools. Global time series of ecosystem and product pool components are shown in Figure 8. The global and regional differences and changes over time of the ecosystem and product carbon pools are compiled for the LULCC and no LULCC simulations in Tables 4 and 5. Global maps of differences in total ecosystem carbon between the experiments are shown at the end of simulations and for the total change over the no LULCC simulations in Figure 9. Additional differences in wood, soil, coarse woody debris, product, leaf, and fine root carbon pools are shown in supporting information Figures S5–S7.

3.2. Historical Land Use Land Cover Change in CESM

The historical LULCC time series is characterized by a global increase in crop area of over 9 million km^2 over the period representing a 184% increase from the 1850 crop area. The increase in crop area corresponds with a 5 million km^2 reduction in tree area, with smaller decreases of 3 million km^2 in grass area and 0.8 million km^2 in shrub area (Figures 1 and 2). These decreases in noncrop PFTs represented reductions of around 10% of their respective 1850 areas (Table 1).

Changes between noncrop vegetation were also seen in response to increases in pasture and changes from primary to secondary land as described in P. J. Lawrence et al. (2012). Global wood harvest rates increased

Table 1
CMIP5 Global and Regional Changes in Area of Land Use and Land Cover Over the Historical and RCP Time Series in CLM4 PFTs (10^6 km^2) and Tree Harvest Area (10^6 km^2/yr)

Time series	Region	Trees	Crop	Grasses	Shrub	Harvest
Historical	Global	−5.10	9.13	−3.21	−0.76	0.11
	North America	−0.84	2.05	−1.13	−0.07	0.02
	South America	−0.89	1.10	−0.12	−0.08	0.00
	Africa	−0.54	1.68	−1.00	−0.11	0.03
	Europe	−0.41	0.80	−0.25	−0.14	0.04
	Russia	−0.52	0.91	−0.38	−0.01	0.01
	Asia	−1.77	2.12	−0.12	−0.21	0.01
	Australia	−0.11	0.47	−0.21	−0.15	0.00
RCP 4.5	Global	2.75	−3.84	0.95	0.15	0.67
	North America	0.56	−0.71	0.15	0.00	0.04
	South America	0.45	−0.45	0.00	0.01	0.02
	Africa	0.31	−0.68	0.34	0.02	0.24
	Europe	0.38	−0.56	0.14	0.04	0.18
	Russia	0.54	−0.79	0.24	0.00	0.03
	Asia	0.46	−0.45	−0.01	0.02	0.16
	Australia	0.05	−0.20	0.10	0.05	0.00
RCP 8.5	Global	−3.45	2.67	0.81	−0.02	1.16
	North America	−0.40	0.23	0.18	−0.02	0.11
	South America	−1.08	0.74	0.36	−0.01	0.19
	Africa	−1.43	1.58	−0.12	0.00	0.41
	Europe	0.02	−0.14	0.11	0.01	0.15
	Russia	−0.09	−0.02	0.11	0.00	0.04
	Asia	−0.21	0.22	−0.02	0.01	0.22
	Australia	−0.25	0.07	0.18	−0.01	0.04

Note. Differences are for the historical (1850 to 2005) and RCP (2006 to 2100) time periods.

dramatically over the period, starting at 0.02 million km^2/yr in 1850 and rising by a factor of 17 to end at 0.37 million km^2/yr in 2005. The cumulative wood harvest area was 17 million km^2, which is over 3 times the area of tree vegetation transformed to another vegetation type.

The LULCC analysis framework shows the Historic impact of LULCC in CESM was to reduce NBP by −0.84 PgC/yr from the positive 0.43 PgC/yr NBP of the no LULCC simulations to a negative −0.41 PgC/yr in the LULCC simulations (Figure 3 and Tables 2 and 3). The reduction in NBP was the result of a Net LULCC of 0.79 PgC/yr, with a cumulative Net LULCC flux to the atmosphere of 123 PgC over the historical period.

The Net LULCC flux was dominated by a large Direct LULCC carbon flux from ecosystems of 0.81 PgC/yr resulting in a cumulative loss of ecosystem carbon of −127 PgC over the period. In addition, there was an Indirect LULCC flux of 0.02 PgC/yr, resulting in a further cumulative carbon loss of −4 PgC. The combined Direct and Indirect LULCC carbon flux was 0.84 PgC/yr resulting in a cumulative loss of ecosystem carbon of −130 PgC over the historical period. This compares to the CESM historical LULCC flux from ecosystems of 127.7 PgC reported in P. J. Lawrence et al. (2012). The Net LULCC flux also included the 0.05 PgC/yr increase in Product Pool Carbon, resulting in a cumulative reduction in the Net LULCC flux by 7 PgC over the period.

The time series analysis (Figure 5) shows that the Direct LULCC started low at 0.15 PgC/yr and increased over the period to end at 1.4 PgC/yr. The Direct LULCC flux out of terrestrial ecosystems was composed equally of conversion fluxes of 0.41 PgC/yr and wood harvest fluxes of 0.41 PgC/yr. There are two distinct spikes in the Direct LULCC over the period corresponding with elevated conversion fluxes from clearing trees for crops in Russia and India over the 1950s and in China over the 1980s.

The historical wood harvest flux simulated in CESM of 0.41 PgC/yr was only 62% of the 0.65 PgC/yr biomass harvest flux prescribed in the CMIP5 LULCC (Hurtt et al., 2011). The CMIP5 wood harvest rates generated by the Global Land Model (GLM) that underpins the LULCC data, however, included a 30% slash component (Hurtt et al., 2011), which is not included in the CESM wood harvest product pool flux. If the slash term is removed from the CMIP5 values, then the equivalent wood harvest flux, which can be compared to CESM1

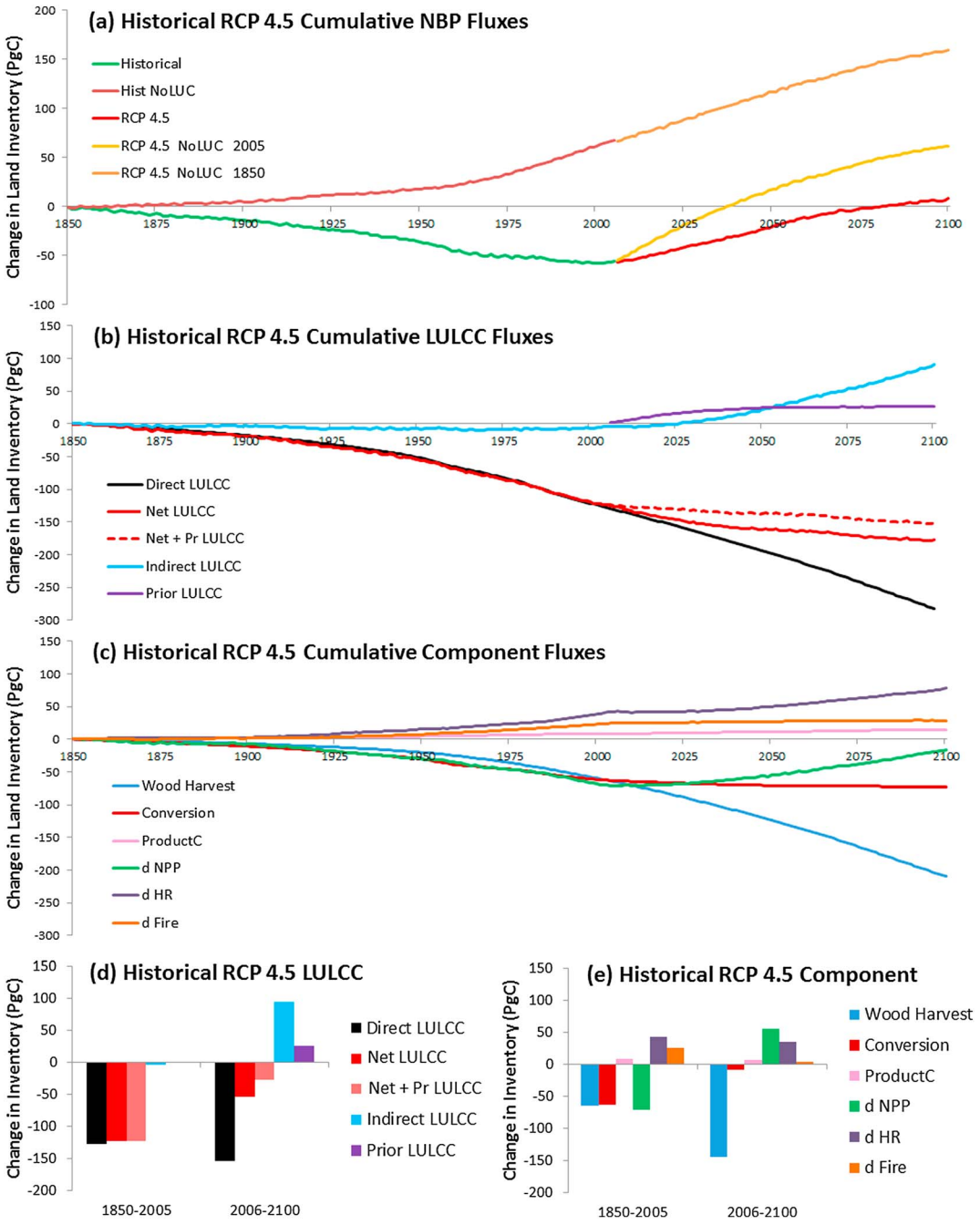

Figure 3. Cumulative NBP and LULCC flux contributions to differences in ecosystem carbon between LULCC and no LULCC simulations for historical and RCP 4.5 periods. Historical no LULCC is taken from 1850 vegetation, and RCP 4.5 no LULCC is taken from 2005 and 1850 vegetation. Historical Prior LULCC flux not included to make the plots consistent with Figure 4 of Mahowald et al. (2016).

results, is 0.50 PgC/yr. This leaves an underestimation of wood harvest in CESM of 0.09 PgC/yr, which corresponds to a cumulative flux difference of 14 PgC compared to the GLM model.

In absolute terms the total ecosystem carbon of the LULCC simulations decreased over the historical period by −61 PgC, with the rate of decrease leveling out to near zero over the last 10 years of the period (Figure 8 and Table 4). The total ecosystem carbon in the no LULCC simulations by contrast increased by 68 PgC, with the rate of increase accelerating from 1970 onward in response to increased NPP from elevated CO_2 and

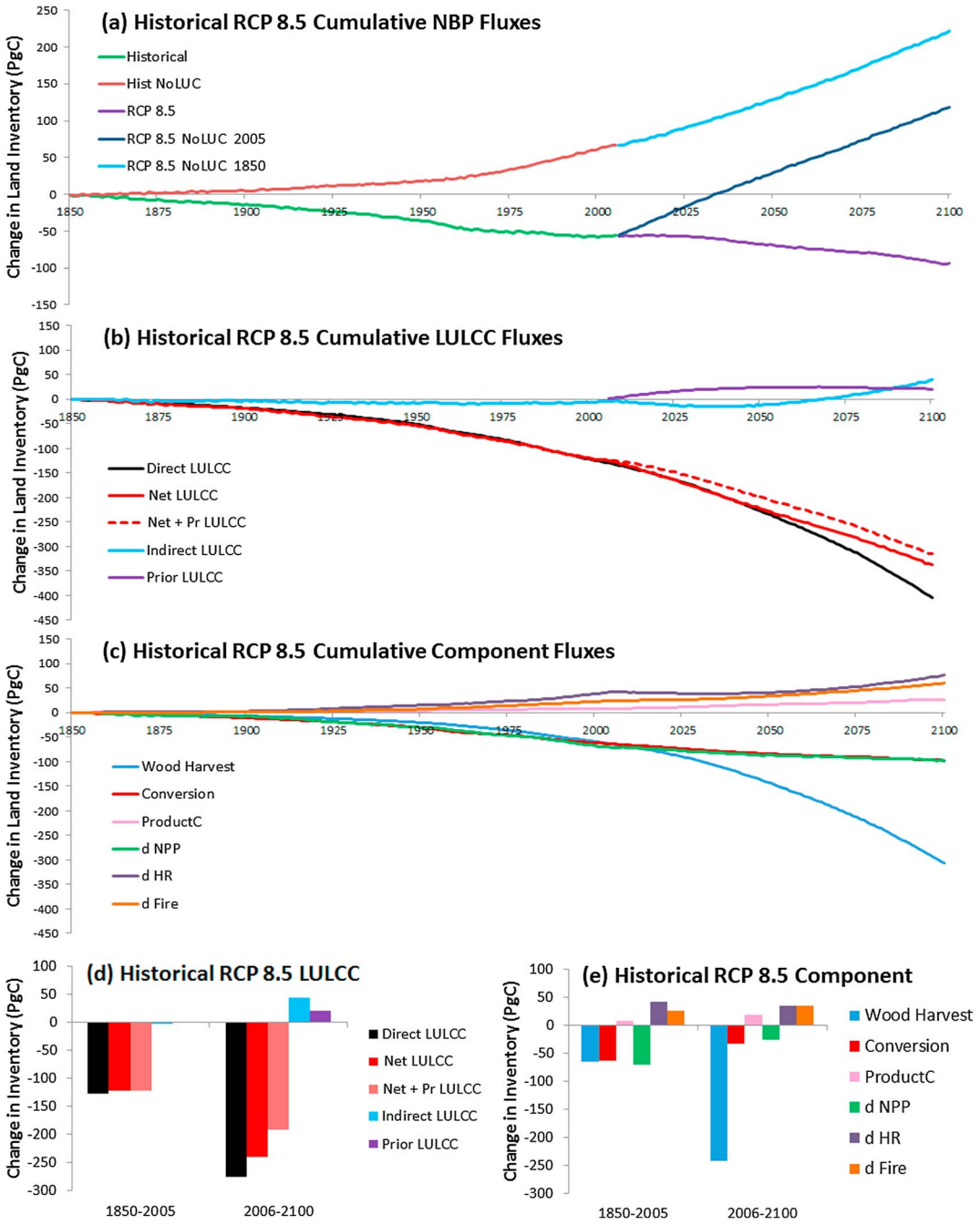

Figure 4. Cumulative NBP and LULCC flux contributions to differences in ecosystem carbon between LULCC and no LULCC simulations for historical and RCP 8.5 periods. Historical no LULCC is taken from 1850 vegetation, and RCP 8.5 no LULCC is taken from 2005 and 1850 vegetation. Historical Prior LULCC flux not included to make the plots consistent with Figure 4 of Mahowald et al. (2016).

changes in climate. This resulted in a difference in total ecosystem carbon (without product pools) between the LULCC and no LULCC simulations of −130 PgC, which was equal to the historical cumulative Direct plus Indirect LULCC flux out of the ecosystem as specified by equation (8) in the analysis framework.

The largest component in the decrease in ecosystem carbon in the historical LULCC simulations was the decrease in wood carbon of −116 PgC, relative to the no LULCC simulations. This alone accounted for 89% of the total ecosystem carbon loss difference between the experiments. The decrease in wood

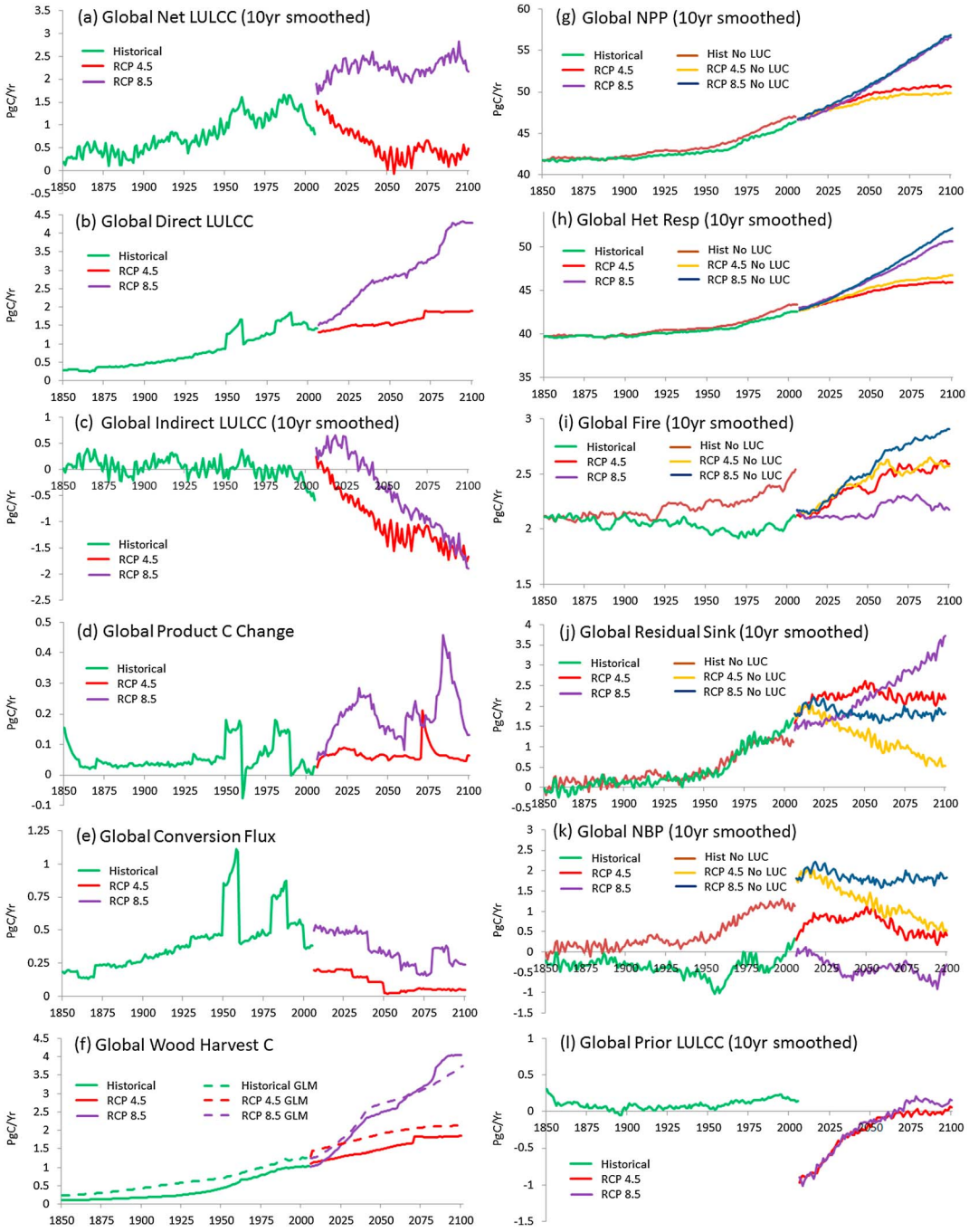

Figure 5. Ensemble mean global time series of fluxes for (a) Net LULCC, (b) Direct LULCC, (c) Indirect LULCC, (d) change in product pools, (e) conversion fluxes from ecosystem, (f) wood harvest, (g) net primary productivity, (h) heterotrophic respiration, (i) fire, (j) residual sink, (k) net biosphere production, and (l) prior LULCC (before 1850 and 1850–2005).

carbon over the historical period in the LULCC simulations was −72 PgC. The increase in wood carbon over the no LULCC experiment by contrast was 44 PgC, accounting for only 64% of the gain in total ecosystem carbon over the period.

The second largest component in the decrease in ecosystem carbon due to LULCC was the reduction in coarse woody debris of −13 PgC, accounting for 10% of total carbon losses. The coarse woody debris of the LULCC simulations decreased by −10 PgC, whereas it increased by 3 PgC in the no LULCC simulations.

Table 2
Ensemble Mean Annual Carbon Fluxes From the LULCC Simulations in PgC/yr

Time series	Region	LULCC direct	LULCC indirect	LULCC Net	LULCC Prior	Convert Total	Wood harvest	Product change	Product decay
Hist	Global	0.81	0.02	0.79	0.11	0.41	0.41	0.05	0.50
	North America	0.14	−0.01	0.11	0.01	0.07	0.07	0.01	0.08
	South America	0.11	−0.01	0.10	0.01	0.06	0.04	0.00	0.06
	Africa	0.13	0.00	0.12	0.01	0.05	0.09	0.01	0.09
	Europe	0.04	0.00	0.04	0.01	0.02	0.02	0.00	0.02
	Russia	0.05	0.01	0.05	0.01	0.02	0.02	0.00	0.03
	Asia	0.33	0.04	0.36	0.06	0.17	0.16	0.02	0.20
	Australia	0.01	0.00	0.01	0.01	0.01	0.00	0.00	0.01
RCP 4.5	Global	1.61	−0.99	0.57	−0.27	0.10	1.51	0.05	1.48
	North America	0.17	−0.13	0.03	−0.05	0.01	0.17	0.01	0.16
	South America	0.24	−0.18	0.05	−0.02	0.01	0.23	0.00	0.23
	Africa	0.45	−0.28	0.17	−0.10	0.01	0.44	0.00	0.44
	Europe	0.05	−0.01	0.03	−0.02	0.00	0.04	0.00	0.04
	Russia	0.08	−0.05	0.02	−0.01	0.01	0.07	0.01	0.07
	Asia	0.59	−0.31	0.26	−0.06	0.06	0.53	0.03	0.52
	Australia	0.02	−0.02	0.01	−0.01	0.00	0.02	0.00	0.02
RCP 8.5	Global	2.86	−0.47	2.23	−0.22	0.35	2.51	0.16	2.47
	North America	0.27	−0.06	0.19	−0.05	0.03	0.24	0.02	0.23
	South America	0.59	−0.07	0.49	−0.02	0.09	0.50	0.03	0.50
	Africa	0.82	−0.04	0.75	−0.10	0.15	0.67	0.03	0.70
	Europe	0.05	0.00	0.05	−0.02	0.00	0.04	0.00	0.04
	Russia	0.11	−0.03	0.07	0.00	0.01	0.10	0.01	0.10
	Asia	0.91	−0.26	0.61	−0.02	0.06	0.85	0.05	0.82
	Australia	0.10	−0.01	0.08	−0.01	0.01	0.10	0.02	0.08

Note. Fluxes are LULCC Direct from Ecosystem, LULCC Indirect, LULCC Net to Atmosphere, LULCC Prior Indirect (before 1850 for historical and from 1850 to 2005 for RCP simulations), conversion flux to atmosphere and product pools, wood harvest to product pools, and product pool change and product pool decay to atmosphere.

Table 3
Ensemble Mean Differences in Annual Carbon Fluxes Between the LULCC and No LULCC Simulations in PgC/yr

Time series	Region	Δ NPP (dt no LUC)	Δ HR (dt no LUC)	Δ fire (dt no LUC)	Δ NEP (dt no LUC)	Δ res sink (dt no LUC)	Δ NBP (dt no LUC)
Historical	Global	−0.46 (5.15)	−0.28 (3.60)	−0.16 (0.34)	−0.18 (1.55)	0.02 (1.21)	−0.84 (1.21)
	North America	−0.11 (0.64)	−0.08 (0.48)	−0.04 (0.07)	−0.02 (0.16)	0.02 (0.10)	−0.12 (0.10)
	South America	−0.04 (0.82)	−0.02 (0.52)	−0.03 (0.14)	−0.03 (0.29)	0.01 (0.15)	−0.10 (0.15)
	Africa	−0.05 (0.95)	−0.03 (0.72)	−0.02 (0.04)	−0.02 (0.23)	0.01 (0.19)	−0.13 (0.19)
	Europe	−0.03 (0.38)	−0.01 (0.28)	−0.01 (0.02)	−0.01 (0.10)	0.00 (0.08)	−0.04 (0.08)
	Russia	−0.05 (0.62)	−0.04 (0.47)	−0.01 (0.02)	−0.01 (0.15)	0.00 (0.13)	−0.05 (0.13)
	Asia	−0.17 (1.60)	−0.09 (1.05)	−0.04 (0.05)	−0.09 (0.56)	−0.02 (0.50)	−0.38 (0.50)
	Australia	−0.01 (0.14)	−0.00 (0.08)	−0.01 (0.00)	−0.00 (0.06)	0.01 (0.06)	−0.01 (0.06)
RCP 4.5	Global	0.58 (2.93)	−0.37 (3.78)	−0.04 (0.46)	0.95 (−0.85)	1.04 (−1.31)	−0.53 (−1.31)
	North America	0.10 (0.42)	−0.04 (0.54)	−0.00 (0.04)	0.13 (−0.12)	0.14 (−0.16)	−0.03 (−0.16)
	South America	0.11 (0.56)	−0.08 (0.61)	0.01 (0.12)	0.20 (−0.05)	0.19 (−0.16)	−0.04 (−0.16)
	Africa	0.17 (0.56)	−0.10 (0.79)	−0.02 (0.12)	0.27 (−0.23)	0.28 (−0.35)	−0.15 (−0.35)
	Europe	−0.03 (0.09)	−0.04 (0.13)	−0.00 (0.02)	0.01 (−0.04)	0.02 (−0.06)	−0.03 (−0.06)
	Russia	0.05 (0.30)	−0.01 (0.38)	−0.00 (0.02)	0.05 (−0.08)	0.06 (−0.10)	−0.02 (−0.10)
	Asia	0.16 (0.91)	−0.11 (1.27)	−0.04 (0.09)	0.27 (−0.36)	0.33 (−0.44)	−0.25 (−0.44)
	Australia	0.01 (0.08)	−0.01 (0.05)	−0.00 (0.05)	0.02 (0.03)	0.02 (−0.03)	−0.01 (−0.03)
RCP 8.5	Global	−0.28 (9.43)	−0.37 (8.80)	−0.37 (0.72)	0.09 (0.63)	0.62 (−0.09)	−2.31 (−0.09)
	North America	−0.01 (1.12)	−0.02 (1.06)	−0.05 (0.11)	0.01 (0.06)	0.08 (−0.05)	−0.20 (−0.05)
	South America	−0.11 (2.06)	−0.08 (1.65)	−0.10 (0.27)	−0.03 (0.42)	0.10 (0.15)	−0.51 (0.15)
	Africa	−0.19 (2.05)	−0.10 (1.96)	−0.14 (0.17)	−0.09 (0.09)	0.07 (−0.08)	−0.76 (−0.08)
	Europe	−0.02 (0.28)	−0.02 (0.31)	−0.01 (0.03)	−0.01 (−0.03)	0.00 (−0.06)	−0.05 (−0.06)
	Russia	0.02 (1.00)	−0.00 (0.95)	−0.01 (0.04)	0.02 (0.05)	0.04 (0.01)	−0.08 (0.01)
	Asia	0.05 (2.51)	−0.14 (2.56)	−0.06 (0.03)	0.19 (−0.05)	0.31 (−0.08)	−0.63 (−0.08)
	Australia	−0.01 (0.41)	−0.00 (0.31)	−0.02 (0.07)	−0.01 (0.10)	0.03 (0.02)	−0.09 (0.02)

Note. Fluxes are net primary production, heterotrophic respiration, fire, net ecosystem production, residual sink, and net biosphere production. Changes in the fluxes over the no LULCC simulation time periods are shown in parentheses.

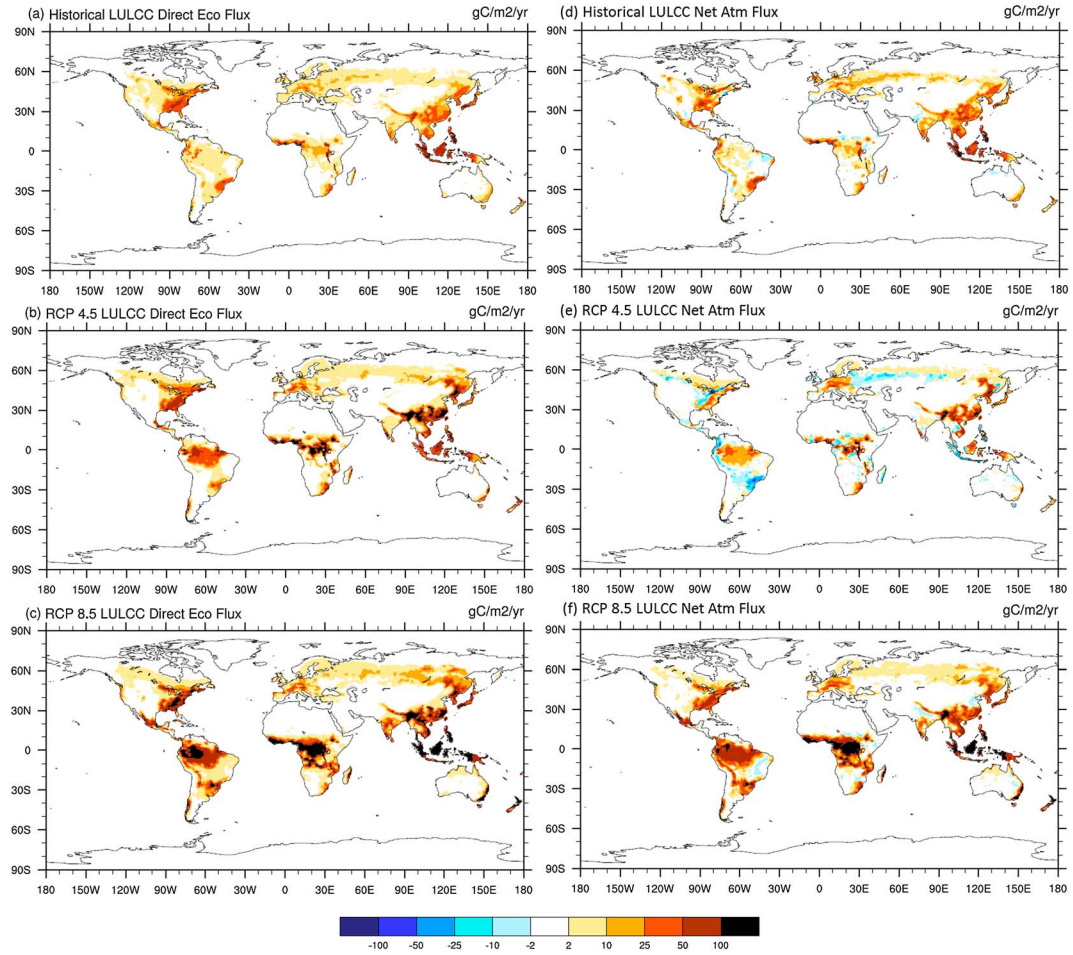

Figure 6. Ensemble average Direct and Net LULCC fluxes from terrestrial ecosystems for historical, RCP 4.5, and RCP 8.5 time periods.

Soil carbon changes were small, with a loss of 3 PgC due to LULCC. Leaf carbon also was lower in the LULCC simulations by −0.6 PgC; however, fine root carbon was increased by 0.2 PgC and litter carbon by 0.2 PgC. The product pool carbon also increased by 7 PgC over the period, being left to be released after the end of the LULCC simulation.

Regionally, the largest Historical Direct plus Indirect LULCC fluxes and corresponding losses of ecosystem carbon were in Asia (−59 PgC), Africa (−20 PgC), North America (−19 PgC), and South America (−16 PgC; Figures 6, 7, and 9 and Tables 2 and 4). In terms of percentages of total ecosystem carbon at the end of the Historical no LULCC simulation, this was ordered as Asia (−18%), North America (−13%), Africa (−8%), and South America (−5%). In Asia and North America the conversion and wood harvest fluxes were equal in size. In Africa wood harvest was almost twice the conversion flux, while in South America the conversion flux was 50% greater than the wood harvest flux.

The Indirect LULCC varied across the regions with Asia showing a positive flux from a decrease in NPP that was larger than the decrease in HR and fire. North and South America, however, exhibited negative Indirect LULCC flux where the fire and HR decreases were larger than the NPP decrease. In all regions the decrease in ecosystem carbon was dominated by the loss of wood carbon. Changes in leaf carbon varied from region to region with South America and Australia both gaining leaf carbon relative to the no LULCC simulations.

Comparison with the Historical Potential Vegetation no LULCC simulations shows that LULCC that occurred before 1850 continued to have an impact in the Historical no LULCC simulations (Figures 5 and 7). The

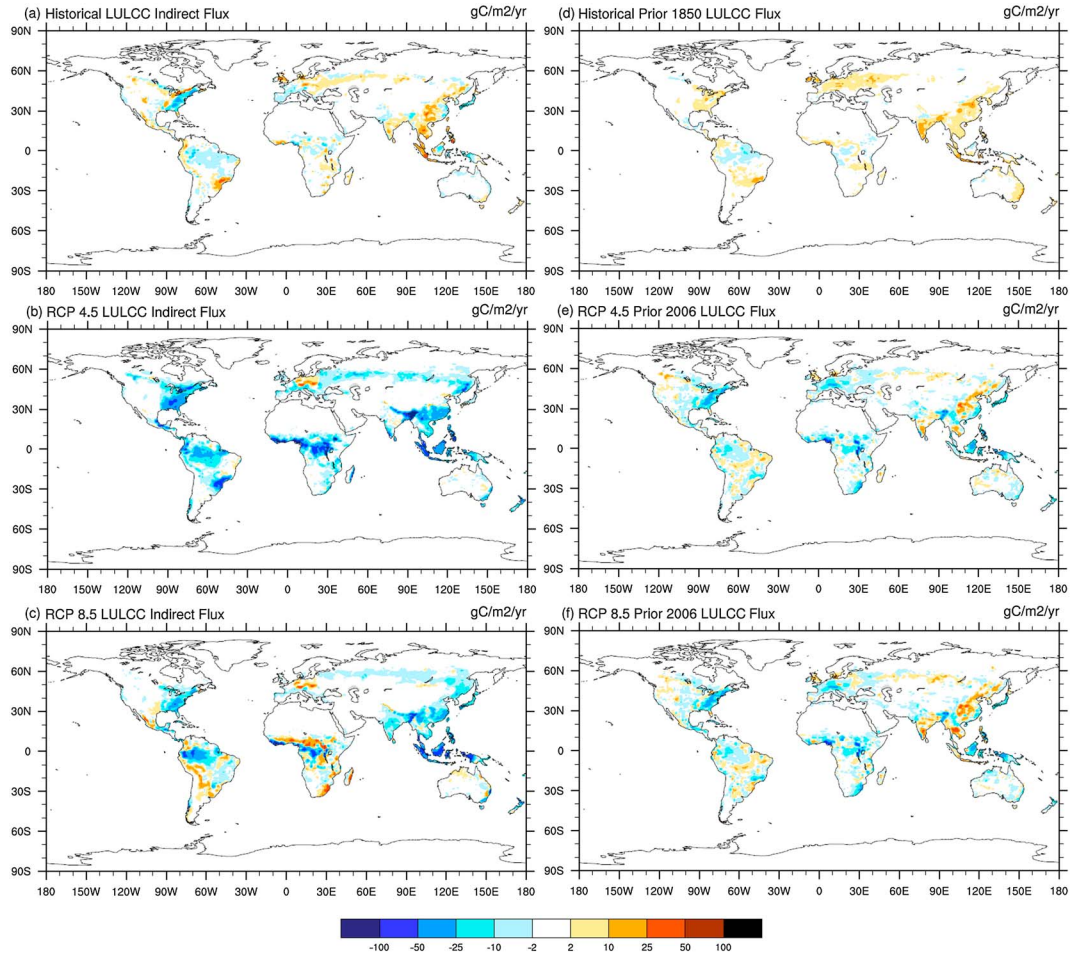

Figure 7. Ensemble average (a–c) Indirect LULCC fluxes and (d–f) Prior LULCC for the historical, RCP 4.5, and RCP 8.5 periods. Prior LULCC is before 1850 for the historical and from 1850 to 2005 for the RCP periods.

impact of this previous LULCC was to reduce potential sinks resulting in a Historical Prior LULCC flux of 0.11 PgC/yr with a cumulative additional loss of 18 PgC from ecosystem carbon compared to the Historical Potential Vegetation no LULCC simulations.

The Historical LULCC simulations also started the simulations with total ecosystem carbon 51 PgC lower than the Historical Potential Vegetation simulations. The Historical Prior LULCC fluxes are not included in the reported Historical LULCC for this study, but this analysis shows that the LULCC prior to 1850 resulted in a further reduction in ecosystem carbon in CESM by 69 PgC at the end of 2005.

3.3. RCP 4.5 Land Use and Land Cover Change in CESM

The CMIP5 RCP 4.5 scenario is characterized as an afforestation scenario (Thomson et al., 2011; van Vuuren et al., 2011). In the CESM time series data this resulted in a large global increase in trees over the period, with a corresponding large decrease in crops and a small increase in grasses (Figures 1 and 2). The increase in trees of 2.75 million km^2 is just over half of the loss of trees of the historical period. The decrease in crops of 3.8 million km^2, however, is just over a third of the increase of crops over the historical period (Table 1).

While this is an afforestation scenario based on the value of carbon stored in forests, global wood harvest area rates are projected in this scenario to continue to increase throughout the 21st century, more than doubling to 0.86 million km^2/yr by 2100. This results in a cumulative wood harvest area of 63 million km^2, which is more than 3 times the cumulative wood harvest area from the historical period. One element of the scenario not

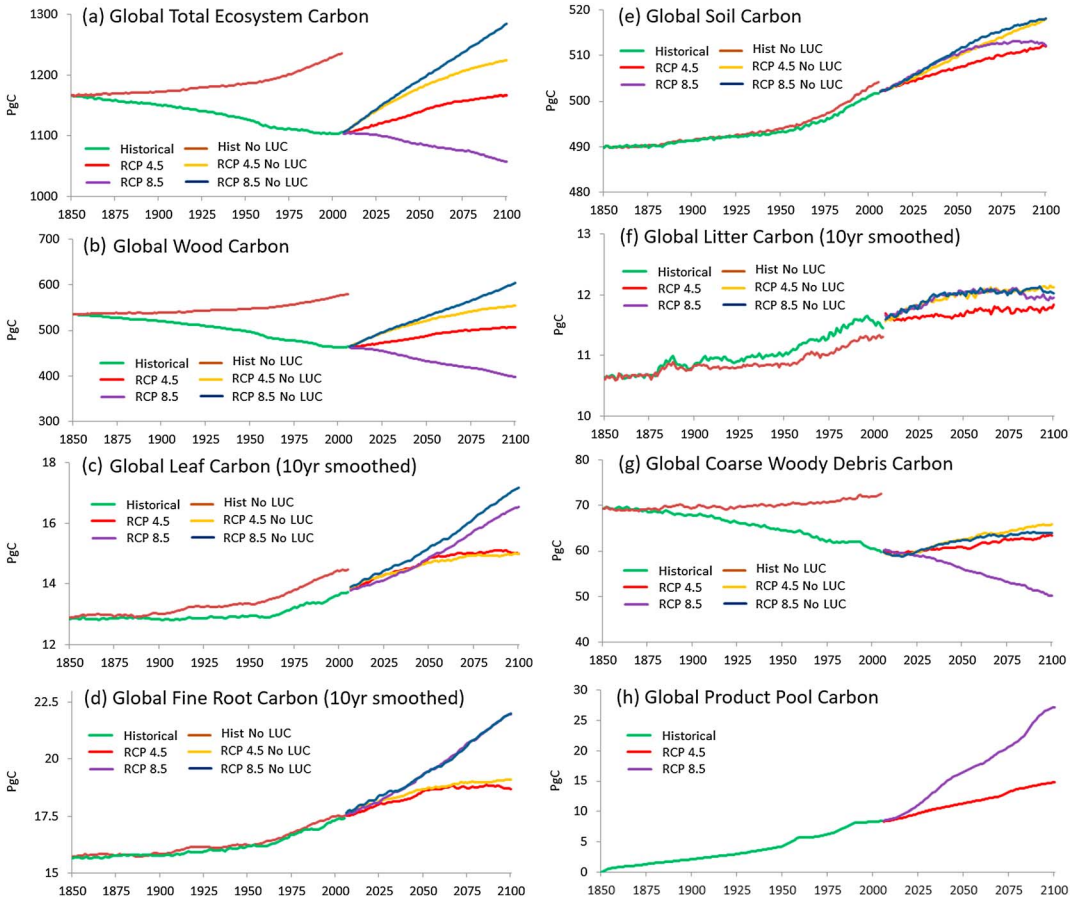

Figure 8. Ensemble mean global time series of carbon pools for (a) total ecosystem carbon, (b) wood carbon, (c) leaf pool carbon, (d) fine root carbon, (e) soil carbon, (f) litter carbon, (g) coarse woody debris, and (h) product pool carbon.

represented in the CESM simulations is bioenergy with carbon capture and storage, which is applied to an increasing fraction of the wood harvested in the second half of the 21st century in the scenario (Thomson et al., 2011).

When the LULCC analysis framework is applied, LULCC in RCP 4.5 is shown to reduce NBP by −0.53 PgC/yr from 1.24 PgC/yr in the no LULCC simulations to 0.72 PgC/yr in the LULCC simulations (Figure 3 and Tables 2 and 3). The reduction in NBP was the result of a Net LULCC of 0.57 PgC/yr, with a cumulative Net LULCC flux to the atmosphere of 53 PgC over the period.

The Net LULCC flux was the result of a large Direct LULCC flux of 1.61 PgC/yr, with a cumulative loss of −153 PgC out of ecosystems (Figure 3 and Table 2). The afforestation combined with higher wood harvest rates produced a large negative Indirect LULCC flux of −0.99 PgC/yr resulting in a cumulative offset of 94 PgC back into terrestrial ecosystems. The combined Direct plus Indirect LULCC flux from ecosystems was 0.62 PgC/yr, representing a cumulative loss of ecosystem carbon of −58 PgC. The Net LULCC flux also included the increase in Product Pool carbon of 0.05 PgC/yr, resulting in a cumulative reduction in the Net LULCC flux by 5 PgC over the period.

The time series analysis (Figure 5) shows that the RCP 4.5 Direct LULCC rates increased gradually through the period starting at 1.3 PgC/yr and ending at 1.8 PgC/yr. The Direct LULCC flux was predominately driven by wood harvest at 1.51 PgC/yr with a much smaller conversion flux of 0.10 PgC/yr. The negative Indirect LULCC flux was the product of higher NPP of 0.58 PgC/yr from afforestation, which combined with lower HR of −0.37 PgC/yr and fire of −0.04 PgC/yr due to higher wood harvest rates that reduced the available ecosystem carbon in the LULCC simulations.

Table 4
Ensemble Mean Changes in Carbon Pools Between LULCC and No LULCC Simulations in PgC for the Last Year of Each Simulation

Time series	Region	Δ Tot eco C (dt no LUC)	Δ wood C (dt no LUC)	Δ soil C (dt no LUC)	Δ CWD C (dt no LUC)
Historical	Global	−129.7 (68.4)	−115.7 (43.5)	−2.5 (14.3)	−12.7 (3.3)
	North America	−19.2 (9.5)	−16.1 (4.8)	−0.7 (2.5)	−2.3 (0.5)
	South America	−15.8 (11.0)	−14.4 (7.9)	0.1 (1.7)	−1.7 (0.8)
	Africa	−20.3 (11.7)	−19.2 (9.0)	0.2 (1.3)	−1.5 (0.1)
	Europe	−6.2 (5.6)	−4.9 (2.1)	−0.4 (2.4)	−0.8 (0.4)
	Russia	−8.0 (7.9)	−6.0 (4.6)	−0.6 (1.5)	−1.1 (0.4)
	Asia	−58.6 (22.3)	−53.3 (14.7)	−1.1 (4.5)	−5.0 (1.1)
	Australia	−1.6 (0.4)	−1.7 (0.4)	0.0 (0.2)	−0.2 (0.0)
RCP 4.5	Global	−57.9 (118.3)	−45.6 (89.6)	−6.0 (15.9)	−2.5 (6.1)
	North America	−3.7 (14.6)	−2.6 (10.6)	−0.9 (2.0)	0.0 (0.9)
	South America	−4.9 (15.4)	−4.2 (12.3)	−0.8 (1.5)	0.5 (0.5)
	Africa	−15.0 (27.6)	−13.2 (23.4)	−1.3 (1.8)	−0.9 (1.4)
	Europe	−3.0 (6.1)	−1.9 (3.1)	−0.7 (2.3)	−0.2 (0.4)
	Russia	−2.4 (10.2)	−2.0 (7.8)	−0.3 (0.6)	−0.2 (0.9)
	Asia	−26.1 (42.1)	−22.2 (30.3)	−1.9 (7.8)	−1.8 (1.7)
	Australia	−0.8 (2.3)	−0.5 (2.1)	−0.1 (−0.2)	0.0 (0.2)
RCP 8.5	Global	−227.0 (177.7)	−204.1 (140.1)	−5.9 (16.0)	−14.8 (4.2)
	North America	−19.1 (19.0)	−16.9 (14.2)	−0.6 (1.7)	−1.8 (0.6)
	South America	−49.7 (28.5)	−45.9 (24.6)	−0.8 (1.2)	−3.2 (−0.1)
	Africa	−71.5 (42.0)	−66.5 (35.6)	−1.2 (1.8)	−4.4 (1.1)
	Europe	−4.6 (8.1)	−3.3 (3.6)	−0.5 (3.1)	−0.4 (0.5)
	Russia	−7.4 (16.0)	−6.1 (12.5)	−0.3 (0.6)	−0.9 (0.7)
	Asia	−61.8 (58.9)	−56.9 (45.3)	−2.4 (7.7)	−3.5 (1.2)
	Australia	−9.0 (5.1)	−8.5 (4.3)	−0.2 (−0.1)	−0.6 (0.3)

Note. Pools are total ecosystem carbon, wood carbon, soil carbon, and coarse woody debris carbon. Differences are between simulations at the end of each time period. Changes in the pools from the start to the end of the simulation time periods are shown in parentheses for the no LULCC simulations.

Table 5
Ensemble Mean Changes in Carbon Pools Between LULCC and No LULCC Simulations in PgC for the Last Year of Each Simulation

Time series	Region	Δ leaf C (dt no LUC)	Δ fine root C (dt no LUC)	Δ litter C (dt no LUC)	Δ product C
Historical	Global	−0.56 (1.48)	0.20 (1.65)	0.18 (0.47)	7.4
	North America	−0.14 (0.37)	−0.04 (0.43)	−0.12 (0.20)	1.3
	South America	0.03 (0.07)	0.17 (0.04)	0.03 (0.01)	0.8
	Africa	−0.06 (0.23)	0.02 (0.29)	0.19 (0.13)	1.4
	Europe	−0.05 (0.13)	0.02 (0.15)	0.03 (0.10)	0.4
	Russia	−0.15 (0.36)	−0.13 (0.38)	−0.01 (0.10)	0.5
	Asia	−0.20 (0.34)	0.13 (0.41)	0.16 (−0.04)	2.9
	Australia	0.02 (−0.02)	0.03 (−0.04)	−0.09 (−0.02)	0.1
RCP 4.5	Global	0.22 (1.13)	−0.09 (1.45)	−0.74 (0.36)	4.8
	North America	−0.01 (0.28)	−0.08 (0.33)	−0.24 (0.30)	0.8
	South America	−0.03 (0.16)	−0.12 (0.21)	−0.02 (0.06)	0.3
	Africa	0.10 (0.12)	0.08 (0.14)	−0.07 (0.08)	0.2
	Europe	0.01 (0.06)	0.00 (0.08)	−0.03 (−0.05)	0.2
	Russia	0.08 (0.24)	0.06 (0.28)	0.01 (−0.09)	0.6
	Asia	0.07 (0.25)	0.02 (0.38)	−0.33 (0.15)	2.5
	Australia	−0.02 (0.02)	−0.04 (0.03)	−0.06 (−0.09)	0.2
RCP 8.5	Global	−0.39 (3.40)	0.25 (4.53)	−0.07 (0.11)	15.1
	North America	−0.05 (0.66)	0.03 (0.85)	0.15 (−0.16)	2.0
	South America	−0.13 (0.60)	−0.01 (0.76)	−0.10 (0.06)	3.1
	Africa	−0.12 (0.56)	0.17 (0.81)	0.30 (0.16)	2.5
	Europe	−0.07 (0.15)	−0.09 (0.20)	−0.02 (0.07)	0.3
	Russia	−0.03 (0.57)	−0.03 (0.65)	−0.08 (−0.08)	1.0
	Asia	0.03 (0.77)	0.18 (1.13)	−0.22 (0.14)	4.6
	Australia	−0.03 (0.09)	0.00 (0.13)	−0.10 (−0.08)	1.6

Note. Pools are leaf carbon, fine root carbon, litter carbon, and change in product pool carbon. Differences are between simulations at the end of each time period. Changes in the pools from the start to the end of the simulation time periods are shown in parentheses for the no LULCC simulations.

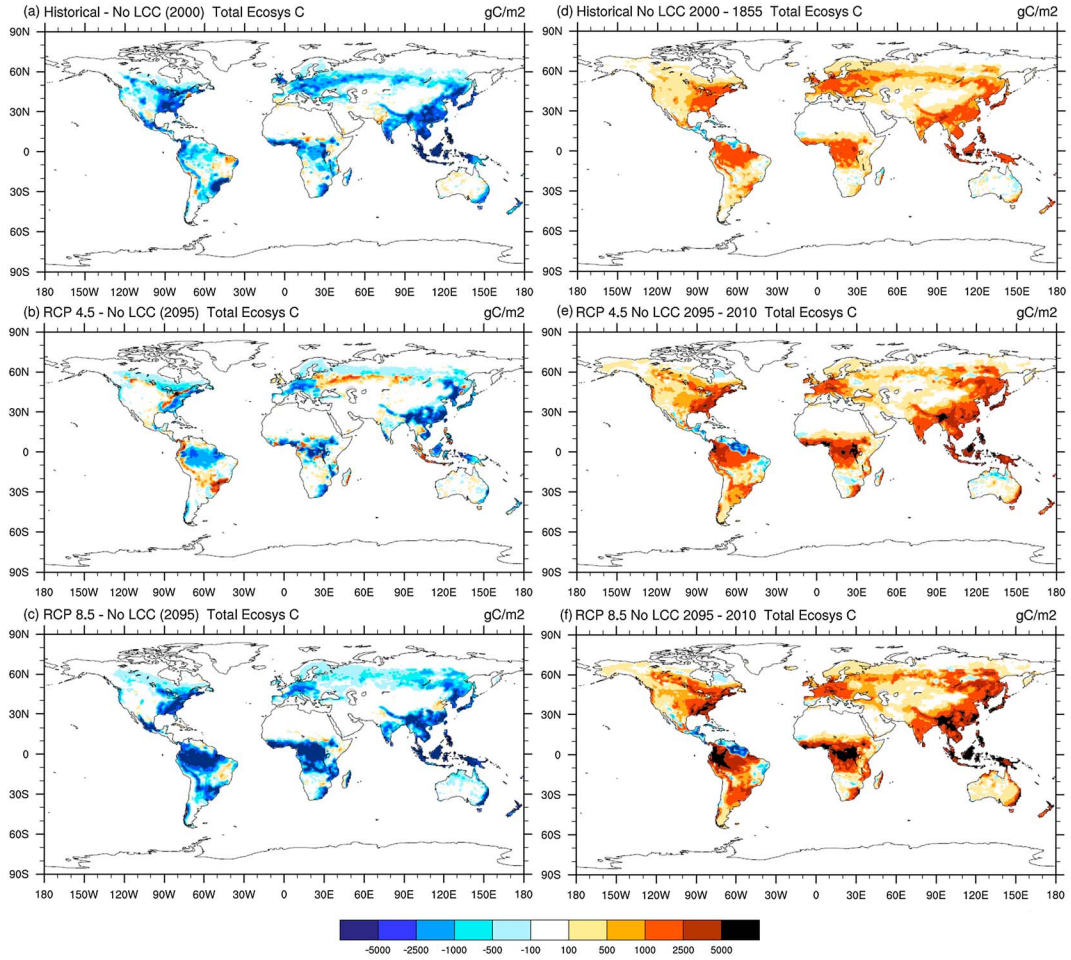

Figure 9. (a–c) Ensemble average difference in Total ecosystem carbon between LULCC and no LULCC simulations at the end of the simulations and (d–f) change over total ecosystem carbon over the no LULCC simulations: historical decades (1850–1859) and (1996–2005) and RCP 4.5 and RCP 8.5 decades (2006–2015) and (2091–2100).

The Indirect LULCC rates become increasingly negative through the period starting at 0.3 PgC/yr and ending at −2.0 PgC/yr. The increase in the size of the negative Indirect LULCC was the result of uptake of carbon from afforestation in the LULCC simulations and the relative reduction in the loss of carbon in the LULCC forests, which were continuously harvested resulting in less ecosystem carbon to be lost through HR and fire.

The Historical LULCC continued to have an influence on the RCP 4.5 no LULCC simulations with a negative Prior LULCC flux of −0.27 PgC/yr, resulting in a cumulative offset of 26 PgC to ecosystems relative to the RCP 4.5 1850 no LULCC simulations. The Prior LULCC flux started very negative at −1.5 PgC/yr and reduces in size to end at 0.1 PgC/yr in 2100. The RCP 4.5 Prior LULCC flux was a combination of Historical reforestation in Eastern North America and Europe and recovering disturbed forests in Africa and South East Asia (Figure 7e).

Including the Prior LULCC flux reduced the Net LULCC further giving an RCP 4.5 Net plus Prior LULCC flux to the atmosphere of 0.30 PgC/yr with a cumulative flux of 27 PgC to the atmosphere relative to the RCP 4.5 1850 no LULCC simulations. The inclusion of the Prior LULCC makes this analysis consistent with the experimental design of Mahowald et al. (2016), which had 1850 vegetation for all no LULCC simulations.

At the end of the RCP 4.5 CESM simulations, the difference in total ecosystem carbon between the LULCC and no LULCC experiments was −58 PgC (Figure 8 and Table 4). The ecosystem carbon in the LULCC simulations

increased by 60 PgC compared to the no LULCC increase of 118 PgC. The loss of ecosystem carbon relative to the no LULCC simulations demonstrates how the higher wood harvest rates were only partially offset by the afforestation in the scenario.

Like the historical simulations, the majority of the difference in ecosystem carbon in RCP 4.5 was in the reduction of wood carbon by 46 PgC in the LULCC simulations. The high wood harvest rates also resulted in reductions in soil carbon of −6 PgC, coarse woody debris of −2 PgC, and litter carbon of −0.7 PgC. The afforestation in the LULCC simulations also resulted in increased leaf carbon of 0.2 PgC but reduced fine root carbon of −0.1 PgC. The product pool carbon increased by 5 PgC over the period to leave 12 PgC in the product pools to be release after the end of the LULCC simulation.

Regionally, the largest RCP 4.5 Direct plus Indirect LULCC fluxes and losses in ecosystem carbon were in Asia (−26 PgC), Africa (−15 PgC), and South America (−5 PgC) with other regions all substantially lower (Figures 6, 7, and 9 and Tables 2 and 4). In terms of percentages of total ecosystem carbon at the end of the RCP 4.5 no LULCC simulation, the order of ecosystem carbon loss was Asia (−8.3%), Europe (−7.6%), and Africa (−5.7%). In all regions wood harvest was the main contribution to Direct LULCC fluxes.

Asia and Africa also had the largest total negative Indirect LULCC fluxes, which were more than 50% of the Direct LULCC fluxes. In North and South America the negative Indirect LULCC fluxes, while smaller, offset over 75% of the Direct LULCC fluxes resulting in Net LULCC fluxes that were less than 25% of the Direct LULCC flux. The majority of the ecosystem carbon losses across all regions were in wood carbon, followed by soil carbon and coarse woody debris.

3.4. RCP 8.5 Land Use Land Cover Change in CESM

The CMIP5 RCP 8.5 scenario is characterized by large increases in cropland and pasture driven by increasing global population (van Vuuren et al., 2011). In the CESM time series data this resulted in a large global increase in crop PFT area, a smaller increase in grass PFT area, and a correspondingly large decrease in tree PFTs (Figure 1 and Table 1). The increase in crop PFT area of 2.7 million km^2 was less than a third of the historical increase in crop PFT and smaller than the decrease in crop PFT of RCP 4.5.

The decrease in tree PFT area of 3.5 million km^2 was more than two thirds of the historical decrease in tree PFTs and larger than the increase in trees PFTs in the RCP 4.5 scenario. Global wood harvest rates increased dramatically over the period to reach 2.3 million km^2/yr by 2100. This was almost 7 times the 2005 value and over twice the RCP 4.5 rate in 2100. This increase resulted in a cumulative wood harvest area of 111 million km^2, which was over 6 times the historical wood harvest area.

Applying the LULCC assessment framework to the high LULCC of RCP 8.5 found that LULCC in RCP 8.5 reduced NBP by −2.31 PgC/yr from 1.84 PgC/yr in the no LULCC simulations to −0.47 PgC/yr in the LULCC simulations (Figure 4 and Tables 2 and 3). The reduction in NBP was the result of a Net LULCC of 2.23 PgC/yr, with a cumulative Net LULCC flux to the atmosphere of 211 PgC over the period.

The Net flux was the product of a large Direct LULCC flux out of the ecosystem of 2.86 PgC/yr, resulting in a cumulative loss of ecosystem carbon of −272 PgC over the period (Figure 4 and Table 2). The loss of ecosystem carbon through wood harvest and conversion fluxes also resulted in a negative Indirect LULCC flux of −0.47 PgC/yr with a cumulative offset of 45 PgC back to ecosystem carbon. The combination of the Direct and Indirect LULCC fluxes was a flux out of the ecosystem of 2.39 PgC/yr with a final cumulative loss of ecosystem carbon of −227 PgC. The Net flux also included the increase in Product Pool carbon of 0.16 PgC/yr, resulting in a cumulative reduction in the Net LULCC flux of 15 PgC over the period.

The time series analysis (Figure 5) showed that RCP 8.5 Direct LULCC increased rapidly over the period from 1.51 PgC/yr in 2006 to 4.28 PgC/yr in 2100. The Direct LULCC flux was dominated by a large wood harvest flux of 2.51 PgC/yr, with a secondary component the conversion flux of 0.35 PgC/yr. The negative Indirect LULCC flux was predominantly due to a decrease in global fire of −0.37 PgC/yr from reduced fuel loads under the high wood harvest rates, with a smaller increase in NEP of 0.09 PgC/yr. The increase in NEP was driven by a large decrease in HR of −0.37 PgC/yr that was larger than the decrease in NPP of −0.28 PgC/yr in the LULCC simulations.

Like in RCP 4.5, the Historical LULCC continued to have an influence on the RCP 8.5 no LULCC simulations with a negative Prior LULCC flux of −0.22 PgC/yr, resulting in a cumulative offset of 20.5 PgC to ecosystems

relative to the RCP 8.5 1850 no LULCC simulations. The RCP 8.5 Prior LULCC flux had the same time evolution as RCP 4.5 starting negative at −1.5 PgC/yr but becoming more positive at the end of the time period at 0.25 PgC/yr in 2100. The spatial pattern for the RCP 8.5 Prior LULCC flux was the same as RCP 4.5 reflecting the same Historical reforestation in Eastern North America and Europe and recovering disturbed forests in Africa and South East Asia (Figure 7f).

When combined with the Net LULCC, this resulted in an RCP 8.5 Net plus Prior LULCC flux of 2.01 PgC/yr and a cumulative flux to the atmosphere of 191 PgC, which was considerably lower than the cumulative Net plus Prior LULCC flux of 250 PgC in Figure 4 of Mahowald et al. (2016). The reason for this difference was that in Mahowald et al. (2016) wood harvest rates were kept at the much higher original CMIP5 RCP 8.5 rate where carbon density discrepancies between the MESSAGE Integrated Assessment Model simulating the scenario and the Global Land Model harmonizing of the land use time series resulted in very large numbers of trees being harvested, as reported in P. J. Lawrence et al. (2012).

At the end of the RCP 8.5 simulations the difference in total ecosystem carbon between the LULCC and no LULCC experiments was −227 PgC (Figure 8 and Table 4). The total ecosystem carbon of the LULCC simulations decreased by −43 PgC, whereas the no LULCC simulations increased by 184 PgC. The majority of the difference in total ecosystem carbon was realized through lower wood carbon in the LULCC simulations of −204 PgC.

The LULCC simulations also had lower coarse woody debris by −15 PgC and lower soil carbon by −6 PgC. The other important carbon pool changes were the decrease in leaf carbon of −0.4 PgC, an increase in fine root carbon of 0.25 PgC, and a decrease in litter carbon of −0.07 PgC. There also was a large increase in product pool carbon of 15 PgC over the period leaving 23 PgC in the product pools to be released after the end of the LULCC simulation.

Regionally, the largest RCP 8.5 Direct plus Indirect LULCC fluxes and losses in ecosystem carbon were in Africa (−72 PgC), Asia (−62 PgC), and South America (−50 PgC), again with all other regions substantially lower (Figures 6, 7, and 9 and Tables 2 and4). In terms of percentages of total ecosystem carbon at the end of the RCP 8.5 no LULCC simulations, the order of carbon loss was Africa (−25.7%), Australia (−24.1%), Asia (−18.7%), and South America (−14.8%). In all regions wood harvest was the main contribution to Direct LULCC fluxes.

Again, the largest regional ecosystem carbon changes were in wood carbon with coarse woody debris and soil carbon making the next contributions. While Africa had the largest ecosystem carbon loss, Asia had the largest wood harvest amount and Direct LULCC flux out of ecosystems. The difference between the two regions was in the Indirect LULCC flux, which was substantially larger in magnitude in Asia at −0.26 PgC/yr than in any other region. The large negative Indirect flux in Asia was driven by an increase in NPP and large decreases in HR and fire in the LULCC simulations compared to the no LULCC simulations.

4. Discussion

4.1. Historical Land Use and Land Cover Change

The CESM historical LULCC and no LULCC simulations showed that the model produced a cumulative Net LULCC flux of 123 PgC to the atmosphere from a Direct LULCC flux of 127 PgC, an Indirect LULCC flux of 4 PgC, and an increase in Product Pools of 7 PgC. The Direct and Indirect LULCC fluxes combined to remove 130 PgC out of the ecosystems over the period. This compares to other global cumulative estimates of around 160 PgC for the period 1850 to 2010, (Arneth et al., 2017; Canadell et al., 2007; Ciais et al., 2014; Houghton, 2003, 2010; D. M. Lawrence et al., 2016).

The analysis showed that CESM underrepresented historical wood harvest by −14 PgC. If the wood harvest in CESM had matched the GLM value, then the additional LULCC flux would have made the cumulative Direct plus Indirect LULCC flux 144 PgC out of ecosystems, and the Net LULCC flux 137 PgC into the atmosphere, bringing these closer with other estimates. Comparison with Historical Potential Vegetation no LULCC simulations also showed that LULCC prior to 1850 had a continued impact on the Historical simulations resulting in a cumulative Prior LULCC flux of 18 PgC, which combined with initial ecosystem carbon that was lower in 1850 by −51 PgC, to have ecosystem carbon that was lower by −69 PgC in 2005.

Despite the low historical wood harvest and Direct LULCC fluxes from the ecosystem, the NBP of the LULCC simulation was negative out of terrestrial ecosystems for all but the last 5 years of the historical simulation. This is in contrast to the positive terrestrial NBP uptake from the 1960s onward reported by a range of independent studies generated with Earth system models, satellite vegetation change inventories, and book keeping methods that account for the land, atmosphere, and ocean sinks in response to LULCC and fossil fuel emissions (Anav et al., 2013; Arneth et al., 2017; Canadell et al., 2007; Ciais et al., 2014; Friedlingstein et al., 2014; Houghton, 2010; Houghton et al., 2012; Le Quere et al., 2009; Le Quere et al., 2015; Pan et al., 2011; Schimel et al., 2015).

The mean of these estimates has a positive NBP of around 1.0 PgC/yr for the 1960 to 2005 period. The main driver of the NBP is a residual sink of around 2.5 PgC/yr. This is offset by a Direct LULCC flux of around 1.5 PgC. While there is a range of uncertainty around these values, the results of these studies are qualitatively similar, with all studies showing increasing NBP arising from an increasingly large residual sink and constant to falling LULCC carbon fluxes over the period.

For the same period CESM had a negative NBP of −0.25 PgC/yr, which starts negative at −0.89 PgC/yr in 1960, reducing in magnitude to zero by 2000, and ending positive at 0.35 PgC/yr in 2005. The overall negative NBP is the result of a much weaker residual sink in CESM of 1.11 PgC/yr over the period. The residual sink starts at 0.33 PgC/yr in 1960 and rises to 1.71 PgC/yr by 2005. Interestingly, the residual sink of the no LULCC simulations over this period also is weak at 1.01 PgC/yr.

While the low LULCC fluxes can be traced to low wood harvest rates, the weak residual sink in CLM4 CN is more complex and is dependent on the terrestrial carbon cycle representation within the model. Anav et al. (2013) and Koven et al. (2013) found that while the CESM BGC model has realistic total vegetation carbon, it had very low soil carbon relative to observational estimates and other Earth system models. They proposed that the low soil carbon and negative NBP of CESM over the end of the historical period were related to the overestimated soil carbon decomposition rates of the model.

The low soil carbon and fast soil carbon turnover rates limit the ability of CLM4 CN to capture changes in soil carbon associated with LULCC and CO_2 fertilization. This is further dampened by the representation of soil biogeochemistry in the model as a single shared soil column for all PFTs in a grid cell. In CLM4 CN all slash fluxes (residues) are transferred to litter and coarse woody debris pools, which in turn decompose and enter the soil through a soil carbon cascade. In line with this, Keppel-Aleks et al. (2013) found that CLM4 had a low residual sink at the end of the historical period, which contributed to the high atmospheric CO_2 concentrations of the fully coupled CESM BGC model.

Further supporting the CLM4 CN carbon cycle investigations, the modeling studies of Friedlingstein et al. (2014) and Arora et al. (2013) show that there is an extremely wide range of responses across CMIP5 Earth system models to elevated CO_2 and climate, even in the absence of LULCC. The idealized 1% CO_2 ramping experiments of Arora et al. (2013) showed that CESM had the weakest carbon uptake of all the CMIP5 models evaluated. The weak carbon uptake that was less than a quarter of other Earth system models was found to be due to the strong nitrogen limitations on productivity increases under the elevated CO_2 (Bonan & Levis, 2010).

4.2. RCP 4.5 Land Use Land Cover Change

For the RCP 4.5 afforestation scenario, CESM produced a cumulative Net LULCC of 53 PgC to the atmosphere from a Direct LULCC flux of 153 PgC, which was offset by a negative Indirect LULCC flux of −94 PgC and an increase in Product Pools of 5 PgC over the period. The combination of the Direct and Indirect LULCC fluxes was a decrease of −58 PgC out of the ecosystem over the period.

The size of the negative Indirect LULCC flux in CESM, however, was affected both by the weak residual sink of CLM4CN and by muted afforestation as represented through the increase in CLM4CN tree PFTs. Di Vittorio et al. (2014) found that the low afforestation area in CESM was due to loss of forest area information in the translation of LULCC from GCAM to the GLM land use model and then to the CLM4CN PFT time series. The lack of forest information was a product of the four GLM land units of the CMIP5 land use time series, with much of the RCP 4.5 afforestation being represented as secondary land in areas that did not currently support forests. The result was that CESM represented only 22% of the increase in forest area that was intended by the GCAM model in the production of the RCP4.5 scenario.

Their study found that in GCAM the forest area of RCP 4.5 increased by 11.0 million km^2, whereas in GLM the increase was reduced to 6.2 million km^2, which was further reduced in CLM to 2.8 million km^2. By passing forest area information, in addition to the four GLM land units used in the CMIP5 LULCC process, the afforestation signal was restored in the CESM simulations of their study. Their analysis showed that this "loss" of afforestation in RCP 4.5 was common across the CMIP5 Earth system models. Di Vittorio et al. (2018) also showed that this level of uncertainty in LULCC mapping can contribute up to 0.5 PgC/yr of uncertainty to LULCC emissions in other time series as well.

The loss of afforestation had large impacts for the RCP 4.5 scenario as the uptake of carbon associated with land management was a large component of the GCAM climate stabilization scenario. Di Vittorio et al. (2014) found that when the afforestation in CESM was forced to reproduce the GCAM values, the uptake of ecosystem carbon was increased by 88 PgC by 2100. This would translate into a decrease in the Net LULCC flux of −1.10 PgC/yr resulting in a cumulative negative Net LULCC flux of −49 PgC/yr in CESM.

Comparison of the CESM RCP 4.5 1850 no LULCC and 2005 no LULCC simulations showed that the Historical LULCC continued to have an impact on the RCP 4.5 no LULCC simulations resulting in a cumulative Prior LULCC flux of −26 PgC. This resulted in a cumulative Net plus Prior LULCC flux of 27 PgC, which was a component not considered in Thomson et al. (2011) or other studies.

4.3. RCP 8.5 Land Use Land Cover Change

For the RCP 8.5 high LULCC scenario, CESM produced a cumulative Net LULCC flux of 211 PgC from a Direct LULCC flux of 272 PgC, which was partially offset by a negative Indirect LULCC flux of −45 PgC and an increase in Product Pools of 15 PgC. The Direct and Indirect LULCC fluxes combined to reduce ecosystem carbon by −227 PgC over the period. The CESM Net LULCC flux of 211 PgC was slightly higher than the cumulative Net LULCC range 25 to 205 PgC calculated in other CMIP5 models (Brovkin et al., 2013; Pongratz et al., 2014).

The very large spread in values across CMIP5 models in the Brovkin et al. (2013) study was traced to whether the individual models included wood harvest in their LULCC processes. The only model in their study that did include wood harvest (JSBACH in MPI-ESM-LR) had the highest ecosystem carbon loss at 205 PgC. These differences reflect the importance of including wood harvest, as it is a primary driver of LULCC fluxes in the RCP 8.5 scenario, which was not captured in the other Earth system models.

While the Net LULCC flux in the MESSAGE model is not reported in Riahi et al. (2011), the scenario is characterized by a large increase in bioenergy predominantly through wood harvest, with some application of bioenergy and carbon capture and storage at the end of the scenario. The large increase in wood harvest was consistent with the CESM RCP 8.5 analysis that found that the wood harvest flux accounted for ~90% of the direct LULCC flux out of terrestrial ecosystems.

As was found in the RCP 4.5 simulations, the Historical LULCC continued to have an impact on the RCP 8.5 no LULCC simulations resulting in a cumulative Prior LULCC flux of −20 PgC. This generated a cumulative Net plus Prior LULCC flux of 191 PgC, which was considerably lower than the cumulative Net plus prior LULCC flux of 250 PgC in Figure 4of Mahowald et al. (2016).

Our results also differ from Mahowald et al. (2016) in that the RCP 8.5 Indirect and Prior LULCC fluxes are both negative offsetting the Direct LULCC fluxes, as opposed to being estimated fractions of the Net plus Prior LULCC fluxes. This underlines the importance of directly attributing the carbon impacts of LULCC from the CESM output files rather than through a process of estimation.

4.4. Other Considerations of Land Use and Land Cover Change in CESM

It has been well established that representing wood harvest is critical for including LULCC in Earth system models, but other land use processes currently absent in CESM and other models also are important (Arneth et al., 2017). One CLM example by Levis et al. (2014) showed that explicit modeling of agricultural practices can affect carbon fluxes, with enhanced carbon emissions through crop harvesting and residue management. Other agricultural activities such as tillage can add additional sources of soil carbon loss when tillage practices are represented.

Agricultural production also results in other greenhouse gas emissions such as CH_4 and N_2O that need to be explicitly accounted for in Earth system models to make them consistent with Integrated Assessment Models. Additionally, including the impacts of shifting cultivation through prescribing the gross LULCC transitions of vegetation can increase cumulative direct LULCC fluxes by 25 to 84 PgC over the historical period, compared to simulations where only net LULCC is prescribed (Arneth et al., 2017; Stocker et al., 2013; Wilkenskjeld et al., 2014).

For CMIP6, some of these issues are being highlighted and evaluated more thoroughly through the Land Use Model Intercomparison Project (D. M. Lawrence et al., 2016). For CESM2, which will be used in CMIP6, we are addressing a number of these missing processes in the new CLM5 model through introduction of (1) wood harvest that is prescribed by carbon amount, rather than area; (2) updated LULCC time series generation methods that utilize the new Land Use Model Intercomparison Project forest area, cropping and grazing data; and (3) transient cropping that is explicitly represented through the CLM crop model with transient nitrogen fertilizer and irrigation (Levis et al., 2012; Sacks et al., 2009). The issues of tillage and shifting cultivation, however, will not be addressed in the release version of CLM5.

Additionally, for CESM simulations in CMIP6, the carbon-nitrogen cycle representation in CLM5 has been updated to better represent state-of-the-science understanding. The new model includes among other revisions (1) vertically resolved soil carbon and nitrogen (Koven et al., 2013), (2) revised photosynthesis and leaf scaling (Bonan et al., 2011), and (3) revised nitrogen cycling dynamics through the Fixation and Uptake of Nitrogen model (Shi et al., 2016), flexible carbon to nitrogen ratios for leaf photosynthetic function (Ghimire et al., 2016), with the benefits of the revised nitrogen representation on the carbon cycle discussed in Wieder et al. (2015).

5. Conclusions

Using an integrated flux and carbon pool assessment framework, we have been able to systematically attribute the carbon cycle impacts of CMIP5 LULCC in CESM to the contributions from individual Direct LULCC actions such as wood harvest and clearing for agriculture and pasture expansion and to a range of Indirect and Prior LULCC actions such as afforestation and the legacy impacts from altered terrestrial sinks from actions that occurred during and before the period of analysis.

Over the historical period CESM produced a cumulative Net LULCC flux of 123 PgC to the atmosphere from a Direct LULCC flux of 127 PgC, an Indirect LULCC flux of 4 PgC, and an increase in Product Pools of 7 PgC. The Direct and Indirect LULCC fluxes combined to remove −130 PgC out of ecosystems. The analysis found that CESM underrepresented the Net LULCC flux compared to other estimates of around 160 PgC (Arneth et al., 2017; Canadell et al., 2007; Ciais et al., 2014; Houghton et al., 2012; D. M. Lawrence et al., 2016).

The analysis found that the low historical LULCC was partially the result of underrepresenting the historical wood harvest by 14 PgC. As has been reported in other studies, CLM4CN has the weakest residual sink of all the CMIP5 models. If the higher Net LULCC flux had been simulated in CESM with this weak residual sink, then the historical NBP would have been further degraded compared with other global estimates.

For the RCP 4.5 scenario, CESM was able to represent some of the mitigation effects of afforestation prescribed by the GCAM model that generated the scenario, with a cumulative Net LULCC flux of 53 PgC to the atmosphere from a Direct LULCC flux of 153 PgC, which was offset by a negative Indirect LULCC flux of −94 PgC, and an increase in Product Pools of 5 PgC. The combination of the Direct and Indirect LULCC fluxes was a decrease of −58 PgC out of the ecosystem.

The LULCC framework showed that the afforestation signal in CESM was substantially lower than prescribed by the GCAM model. Di Vittorio et al. (2014) found that when the afforestation in CESM was forced to reproduce the GCAM values, the uptake of ecosystem carbon was increased by 88 PgC by 2100.

For the RCP 8.5 high LULCC scenario, CESM produced a cumulative Net LULCC flux of 211 PgC to the atmosphere from a Direct LULCC flux of 272 PgC, which was partially offset by a negative Indirect LULCC flux of −45 PgC and an increase in Product Pools of 15 PgC. The Direct and Indirect LULCC fluxes combined to reduce ecosystem carbon by −227 PgC. The large Direct and Net LULCC fluxes in CESM were consistent

with the large increase in bioenergy from wood harvest prescribed by the MESSAGE model for the scenario (Riahi et al., 2011).

Comparison of the CESM results to the RCP 8.5 LULCC fluxes simulated in other CMIP5 models showed that all Earth system models that did not include wood harvest grossly underrepresented the LULCC of this scenario (Brovkin et al., 2013). The LULCC analysis framework also showed that CESM RCP 8.5 Indirect and Prior LULCC fluxes are negative and offset Direct LULCC fluxes, as opposed to being fractions of the Net plus Prior LULCC fluxes as estimated in Mahowald et al. (2016).

Acknowledgments
This work was supported by the National Center for Atmospheric Research, Community Earth System Model (CESM) Land and Biogeochemistry Working Groups, and the Weather and Climate Impact Assessment Science Initiative, which are all sponsored by the National Science Foundation. Thanks also are due to the software engineers and scientists who worked on developing CESM and to the Computational and Information Systems Laboratory at NCAR, which provided the computing resources through the Climate Simulation Laboratory. This work also was supported for P. J. L. by the National Science Foundation grant AGS-1243095 and for D. M. L. by the U.S. Department of Energy grants DE-FC03-97ER62402/A010 and DE-SC0012972 and U.S. Department of Agriculture grant 2015-67003-23489. The CESM model and the land surface data sets used in this paper are available for public access at the NCAR CESM website http://www.cesm.ucar.edu/.

References

Anav, A., Friedlingstein, P., Kidston, M., Bopp, L., Ciais, P., Cox, P., et al. (2013). Evaluating the land and ocean components of the global carbon cycle in the CMIP5 Earth System Models. *Journal of Climate*, *26*(18), 6801–6843. https://doi.org/10.1175/JCLI-D-1112-00417.00411

Arneth, A., Sitch, S., Pongratz, J., Stocker, B. D., Ciais, P., Poulter, B., et al. (2017). Historical carbon dioxide emissions caused by land-use changes are possibly larger than assumed. *Nature Geoscience*, *10*(2), 79–84. https://doi.org/10.1038/NGEO2882

Arora, V. K., & Boer, G. J. (2010). Uncertainties in the 20th century carbon budget associated with land use change. *Global Change Biology*, *16*(12), 3327–3348. https://doi.org/10.1111/j.1365-2486.2010.02202.x

Arora, V. K., Boer, G. J., Friedlingstein, P., Eby, M., Jones, C. D., Christian, J. R., et al. (2013). Carbon–concentration and carbon–climate feedbacks in CMIP5 Earth System Models. *Journal of Climate*, *26*(15), 5289–5314. https://doi.org/10.1175/JCLI-D-1112-00494.00491

Bonan, G. B., Lawrence, P. J., Oleson, K. W., Levis, S., Jung, M., Reichstein, M., et al. (2011). Improving canopy processes in the Community Land Model version 4 (CLM4) using global flux fields empirically inferred from FLUXNET data. *Journal of Geophysical Research*, *116*, G02014. https://doi.org/10.1029/2010JG001593

Bonan, G. B., & Levis, S. (2010). Quantifying carbon-nitrogen feedbacks in the Community Land Model (CLM4). *Geophysical Research Letters*, *37*, L07401. https://doi.org/10.1029/2010GL042430

Brovkin, V., Boysen, L., Arora, V. K., Boisier, J. P., Cadule, P., Chini, L., et al. (2013). Effect of anthropogenic land-use and land-cover changes on climate and land carbon storage in CMIP5 projections for the twenty-first century. *Journal of Climate*, *26*(18), 6859–6881. https://doi.org/10.1175/JCLI-D-1112-00623.00621

Canadell, J. G., Le Quere, C., Raupach, M. R., Field, C. B., Buitenhuis, E. T., Ciais, P., et al. (2007). Contributions to accelerating atmospheric CO_2 growth from economic activity, carbon intensity, and efficiency of natural sinks. *Proceedings of the National Academy of Sciences*, *104*, 18,866–18,870.

Canadell, J. G., & Schulze, E. D. (2014). Global potential of biospheric carbon management for climate mitigation. *Nature Communications*, *5*, 5282. https://doi.org/10.1038/ncomms6282

Ciais, P., Sabine, C., Bala, G., Bopp, L., Brovkin, V., Canadell, J., et al. (2014). Carbon and other biogeochemical cycles. In *Climate Change 2013: The Physical Science Basis. Contribution of Working Group I to the Fifth Assessment Report of the Intergovernmental Panel on Climate Change* (pp. 465–570). Cambridge University Press.

Di Vittorio, A. V., Chini, L. P., Bond-Lamberty, B., Mao, J., Shi, X., Truesdale, J., et al. (2014). From land use to land cover: Restoring the afforestation signal in a coupled integrated assessment-earth system model and the implications for CMIP5 RCP simulations. *Biogeosciences*, *11*(22), 6435–6450. https://doi.org/10.5194/bg-5111-6435-2014

Di Vittorio, A. V., Mao, J., Shi, X., Chini, L., Hurtt, G., & Collins, W. D. (2018). Quantifying the effects of historical land cover conversion uncertainty on global carbon and climate estimates. *Geophysical Research Letters*, *45*, 974–982. https://doi.org/10.1002/2017GL075124

Friedlingstein, P., Meinshausen, M., Arora, V. K., Jones, C. D., Anav, A., Liddicoat, S. K., & Knutti, R. (2014). Uncertainties in CMIP5 climate projections due to carbon cycle feedbacks. *Journal of Climate*, *27*(2), 511–526. https://doi.org/10.1175/JCLI-D-1112-00579.00571

Gasser, T., & Ciais, P. (2013). A theoretical framework for the net land-to-atmosphere CO_2 flux and its implications in the definition of "emissions from land-use-change". *Earth System Dynamics*, *4*, 171–186. https://doi.org/10.5194/esd-5194-5171-2013

Gent, P. R., & Danabasoglu, G. (2011). The community climate system model version 4. *Journal of Climate*, *24*(19), 4992–4998. https://doi.org/10.1175/JCLI-D-10-05011.1

Ghimire, B., Riley, W. J., Koven, C. D., Mu, M., & Randerson, J. T. (2016). Representing leaf and root physiological traits in CLM improves global carbon and nitrogen cycling predictions. *Journal of Advances in Modeling Earth Systems*, *8*(2), 598–613. https://doi.org/10.1002/2015MS000538

Houghton, R. A. (2003). Revised estimates of the annual net flux of carbon to the atmosphere from changes in land use and land management 1850–2000. *Tellus*, *55*(2), 378–390. https://doi.org/10.1034/j.1600%E2%80%930889.2003.01450.x

Houghton, R. A. (2010). How well do we know the flux of CO_2 from land-use change. *Tellus*, *62B*. https://doi.org/10.1111/j.1600-0889.2010.00473

Houghton, R. A., House, J. I., Pongratz, J., van der Werf, G. R., DeFries, R. S., Hansen, M. C., et al. (2012). Carbon emissions from land use and land-cover change. *Biogeosciences*, *9*(12), 5125–5142. https://doi.org/10.5194/bg-9-5125-2012

Hurtt, G. C., Chini, L. P., Frolking, S., Betts, R. A., Feddema, J., Fischer, G., et al. (2011). Harmonization of land-use scenarios for the period 1500-2100: 600 years of global gridded annual land-use transitions, wood harvest, and resulting secondary lands. *Climatic Change*, *109*(1-2), 117–161. https://doi.org/10.1007/s10584-011-0153-2

Keppel-Aleks, G., Randerson, J. T., Lindsay, K., Stephens, B. B., Keith Moore, J., Doney, S. C., et al. (2013). Atmospheric carbon dioxide variability in the Community Earth System Model: Evaluation and transient dynamics during the twentieth and twenty-first centuries. *Journal of Climate*, *26*(13), 4447–4475. https://doi.org/10.1175/JCLI-D-1112-00589.00581

Koven, C. D., Riley, W. J., Subin, Z. M., Tang, J. Y., Torn, M. S., Collins, W. D., et al. (2013). The effect of vertically resolved soil biogeochemistry and alternate soil C and N models on C dynamics of CLM4. *Biogeosciences*, *10*(11), 7109–7131. https://doi.org/10.5194/bg-5110-7109-2013

Landrum, L., Otto-Bliesner, B. L., Conley, A., Lawrence, P. J., Rosenbloom, N., & Teng, H. (2013). Last millennium climate and its variability in CCSM4. *Journal of Climate*, *26*(4), 1085–1111. https://doi.org/10.1175/JCLI-D-1111-00326.00321

Lawrence, D. M., Hurtt, G. C., Arneth, A., Brovkin, V., Calvin, K. V., Jones, A. D., et al. (2016). The Land Use Model Intercomparison Project (LUMIP): Rationale and experimental design. *Geoscientific Model Development*, *9*(9), 2973–2998. https://doi.org/10.5194/gmd-5199-2973-2016

Lawrence, D. M., Oleson, K. W., Flanner, M. G., Fletcher, C. G., Lawrence, P. J., Levis, S., et al. (2012). The CCSM4 land simulation, 1850-2005: Assessment of surface climate and new capabilities. *Journal of Climate*, *25*(7), 2240–2260. https://doi.org/10.1175/JCLI-D-1111-00103.00101

Lawrence, P. J., Feddema, J. J., Bonan, G. B., Meehl, G. A., O'Neill, B. C., Oleson, K. W., et al. (2012). Simulating the biogeochemical and biogeophysical impacts of transient land cover change and wood harvest in the Community Climate System Model (CCSM4) from 1850 to 2100. *Journal of Climate*, *25*(9), 3071–3095. https://doi.org/10.1175/JCLI-D-11-00256.1

Le Quere, C., Moriarty, R., Andrew, R. M., Canadell, J. G., Sitch, S., Korsbakken, J. I., et al. (2015). Global carbon budget 2015. *Earth System Science Data*, *7*(2), 349–396. https://doi.org/10.5194/essd-5197-5349-2015

Le Quere, C., Raupach, M. R., Canadell, J. G., Marland, G., Bopp, L., Ciais, P., et al. (2009). Trends in the sources and sinks of carbon dioxide. *Nature Geoscience*, *6*(1), 6. https://doi.org/10.1038/ngeo1689

Levis, S., Bonan, G. B., Kluzek, E., Thornton, P. E., Jones, A., Sacks, W. J., & Kucharik, C. J. (2012). Interactive crop management in the Community Earth System Model (CESM1): Seasonal influences on land–atmosphere fluxes. *Journal of Climate*, *25*(14), 4839–4859. https://doi.org/10.1175/JCLI-D-1111-00446.00441

Levis, S., Hartman, M. D., & Bonan, G. B. (2014). The Community Land Model underestimates land-use CO_2 emissions by neglecting soil disturbance from cultivation. *Geoscientific Model Development*, *7*(2), 613–620. https://doi.org/10.5194/gmd-5197-5613-2014

Lindsay, K., Bonan, G. B., Doney, S. C., Hoffman, F. M., Lawrence, D. M., Long, M. C., et al. (2014). Preindustrial-control and twentieth-century carbon cycle experiments with the Earth System Model CESM1(BGC). *Journal of Climate*, *27*(24), 8981–9005. https://doi.org/10.1175/JCLI-D-1112-00565.00561

Mahowald, N. M., Randerson, J. T., Lindsay, K., Munoz, E., Doney, S. C., Lawrence, P., et al. (2016). Interactions between land use change and carbon cycle feedbacks. *Global Biogeochemical Cycles*, *31*, 96–113. https://doi.org/10.1002/2016GB005374

Pan, Y., Birdsey, R. A., Fang, J., Houghton, R., Kauppi, P. E., Kurz, W. A., et al. (2011). A large and persistent carbon sink in the world's forests. *Science*, *333*(6045), 988–993. https://doi.org/10.1126/science.1201609

Pongratz, J., Reick, C. H., Houghton, R. A., & House, J. I. (2014). Terminology as a key uncertainty in net land use and land cover change carbon flux estimates. *Earth System Dynamics*, *5*(1), 177–195. https://doi.org/10.5194/esd-5195-5177-2014

Riahi, K., Rao, S., Krey, V., Cho, C., Chirkov, V., Fischer, G., et al. (2011). RCP 8.5—A scenario of comparatively high greenhouse gas emissions. *Climatic Change*, *109*(1-2), 33–57. https://doi.org/10.1007/s10584-10011-10149-y

Sacks, W. J., Cook, B. I., Buenning, N., Levis, S., & Helkowski, J. H. (2009). Effects of global irrigation on the near-surface climate. *Climate Dynamics*, *33*, 159–175. https://doi.org/10.1007/s00382%E2%80%9300008-00445-z

Schimel, D., Stephens, B. B., & Fisher, J. B. (2015). Effect of increasing CO_2 on the terrestrial carbon cycle. *Proceedings of the National Academy of Sciences*, *112*(2), 436–441. https://doi.org/10.1073/pnas.1407302112

Shi, M., Fisher, J. B., Brzostek, E. R., & Phillips, R. P. (2016). Carbon cost of plant nitrogen acquisition: Global carbon cycle impact from an improved plant nitrogen cycle in the Community Land Model. *Global Change Biology*, *22*(3), 1299–1314. https://doi.org/10.1111/gcb.13131

Smith, P., Haberl, H., Popp, A., Erb, K. H., Lauk, C., Harper, R., et al. (2013). How much land-based greenhouse gas mitigation can be achieved without compromising food security and environmental goals? *Global Change Biology*, *19*(8), 2285–2302. https://doi.org/10.1111/gcb.12160

Stocker, B. D., Feissli, F., Strassmann, K. M., Spahni, R., & Joos, F. (2013). Past and future carbon fluxes from land use change, shifting cultivation and wood harvest. *Tellus*, *66*. https://doi.org/10.3402/tellusb.v3466.23188

Taylor, K. E., Stouffer, R. J., & Meehl, G. A. (2009). A Summary of the CMIP5 experiment design (Rep.pp. 1-32), World Climate Research Program.

Thomson, A. M., Calvin, K. V., Smith, S. J., Kyle, G. P., Volke, A., Patel, P., et al. (2011). RCP4.5: A pathway for stabilization of radiatve forcing by 2100. *Climatic Change*, *109*(1-2), 77–94. https://doi.org/10.1007/s10584-10011-10151-10584

van der Werf, G. R., Morton, D. C., DeFries, R. S., Olivier, J. G. J., Kasibhatla, P. S., Jackson, R. B., et al. (2009). CO_2 emissions from forest loss. *Nature Geoscience*, *6*(2), 139–145. https://doi.org/10.1038/ngeo1671

Van Vuuren, D., Edmonds, J., Kainuma, M., Riahi, K., Thomson, A., Hibbard, K., et al. (2011). The representative concentration pathways: An overview. *Climatic Change*, *109*(1-2), 5–31. https://doi.org/10.1007/s10584-011-0148-z

Watson, R. T., Nobel, I. R., Bolin, B., Ravindranath, N. H., Verado, D. J., & Dokken, D. J. (2000). *Land use, land-use change and forestry* (p. 375). Cambridge, UK: IPCC.

Wieder, W. R., Cleveland, C. C., Lawrence, D. M., & Bonan, G. B. (2015). Effects of model structural uncertainty on carbon cycle projections: Biological nitrogen fixation as a case study. *Environmental Research Letters*, *10*(4). https://doi.org/10.1088/1748-9326/1010/1084/044016

Wilkenskjeld, S., Kloster, S., Pongratz, J., Raddatz, T., & Reick, C. H. (2014). Comparing the influence of net and gross anthropogenic land-use and land-cover changes on the carbon cycle in the MPI-ESM. *Biogeosciences*, *11*(17), 4817–4828. https://doi.org/10.5194/bg-5111-4817-2014